



Quaternary Glaciation in the Mountains of Crete, Greece

Aris D. Leontaritis ^{a,b,*}, Daniel Moraetis ^c, Kosmas Pavlopoulos ^d, Philip D. Hughes ^e, Charalampos Fassoulas ^{f,g}

^a National and Kapodistrian University of Athens, Greece

^b The Greek Mountain Project, Greece

^c University of Sharjah, United Arab Emirates

^d Sorbonne University Abu Dhabi, SAFIR, United Arab Emirates

^e The University of Manchester, UK

^f Psiloritis UNESCO Global Geopark, Greece

^g Natural History Museum of Crete, Greece

ARTICLE INFO

Keywords:

Quaternary
Glaciation
Greece
Crete
Mt Ida
Lefka Ori
Mediterranean

ABSTRACT

This study reviews the Quaternary glacial record of the mountains of Crete, aiming to resolve existing uncertainties and evaluate its regional paleoclimatic implications. We present the results of extensive fieldwork conducted in the Ida (2456 m a.s.l.) and Lefka Ori massifs (2453m a.s.l.), alongside a critical review of related geomorphological and sedimentary studies. Evidence suggests a strong dependence on local topoclimatic factors, reflecting marginal conditions for glaciation, with reconstructed regional Equilibrium Line Altitudes ranging from approximately 2070 to 2100 m a.s.l. On Mt. Ida, we mapped a glacial sequence within a typical cirque–moraine system. Three distinct glacial phases were identified and tentatively correlated with the Middle Pleistocene (Marine Isotope Stages [MIS] 12 and 6) and the Last Glacial Maximum (LGM, MIS2) upon correlations with the glacial chronostratigraphy in mainland Greece. At a broader paleoclimatic scale, absolute dating of the stratigraphically youngest glacial phase on Mt. Ida would strengthen the hypothesis of wetter climatic conditions in southern Greece and western Turkey during the LGM, potentially driven by paleoatmospheric circulation patterns that supplied moisture along a more southwest-northeast trajectory than at present. Notably, prominent glacial features are absent from the Lefka Ori massif, despite being both larger and currently wetter than Mt. Ida. Preliminary geomorphological analysis suggests that this contrast is primarily due to the lack of topographic configurations conducive to ice accumulation in the highlands of Lefka Ori. Tectonic factors also appear to have played a key role. Variations in tectonic uplift timing and rates suggest that Lefka Ori accumulated more uplift during the Late Quaternary, while Mt. Ida experienced greater uplift prior to the Middle Pleistocene, likely influencing paleo-elevations during glacial periods. Given the marginal conditions for glaciation and high ELAs, these three factors—topography, atmospheric circulation, and tectonic history—likely played critical roles in glacier formation on Crete.

1. Introduction

1.1. The Quaternary glacial history of Greece

Evidence of Quaternary glaciation is abundant among mountains in mainland Greece exceeding 1800 m in elevation (Fig. 1; Niculescu, 1915; Mistardis, 1937; Hughes et al., 2006a; Styllas et al., 2018; Leontaritis et al., 2020 and references therein). The largest glaciations in Greece occurred during the Middle Pleistocene, specifically during the

Skamnelli Stage (Marine Isotope Stage [MIS] 12) and the Vlasian Stage (MIS 6), as indicated by Uranium series (U-series) dating of moraines on Mt. Tymphi in the North Pindus mountains (Fig. 1; Woodward et al., 2004; Hughes et al., 2006a) and strengthened by sedimentological analyses combined with U-series and Optically Stimulated Luminescence (OSL) dating of glaciofluvial outwash fans in Mt. Chelmos (Pope et al., 2023). The general trend of larger Middle Pleistocene glaciations compared to the Late Pleistocene aligns with findings from other regions in the Balkans, such as Montenegro (Hughes et al., 2010, 2011) and

* Corresponding author. National and Kapodistrian University of Athens, Department of Geology and Geoenvironment, Panepistimiopolis, Zografou Athens, 15784, Greece.

E-mail address: leontari@geol.uoa.gr (A.D. Leontaritis).

Croatia (Marjanac and Marjanac, 2016). The study on Mt. Chelmos also presents evidence for an extensive MIS 16 glaciation (Pope et al., 2023).

Glaciers were likely present during every cold stage, although the glacial record preserves evidence of successively smaller glaciations. For example, the glaciers of the Vlasian Stage (MIS 6) were smaller than those of the Skamnelli Stage (MIS 12). Evidence of even older and more extensive glaciations is rare. On Mt. Chelmos, U-series ages of cemented tillite suggest an earlier glaciation linked to MIS 16, tentatively named the Valvousian Stage based on the regional chronostratigraphical cold stage classification (Pope et al., 2023). However, additional data is required to consolidate this. Extensive ice caps formed on Mt. Tymphi and Mt. Chelmos, with glaciers on all slope orientations during the most extensive phases (Pope et al., 2017; Leontaritis et al., 2020). Similar ice configurations likely occurred on high-elevation

massifs (>2200 m) in mainland Greece, such as Mt. Smolikas, Mt. Lakmos, Mt. Vardousia, and Mt. Parnassus (Fig. 1). A useful measure for comparing paleoglaciers is the Equilibrium Line Altitude (ELA), where annual accumulation and ablation balance, and is governed by air temperature and precipitation (Ohmura and Boettcher, 2018). Using the Accumulation Area Ratio (AAR) method with a ratio of 0.6 to estimate ELAs, glaciers from MIS 12 had average ELAs of 1741 m a.s.l. on Mt. Tymphi and 1680 m a.s.l. on Mt. Smolikas (Hughes, 2004), and 1967 m a.s.l. on Mt. Chelmos (Pope et al., 2017). This 220–280 m difference reflects a warmer, drier climate in the Peloponnese, consistent with their 2° latitude difference (Pope et al., 2017).

Ice extent was significantly smaller during the Last Glacial Cycle (MIS 5d-2), and even during the LGM (27.5–23.3 ka; Hughes and Gibbard, 2015) glaciers were confined to high valleys and cirques (Pope

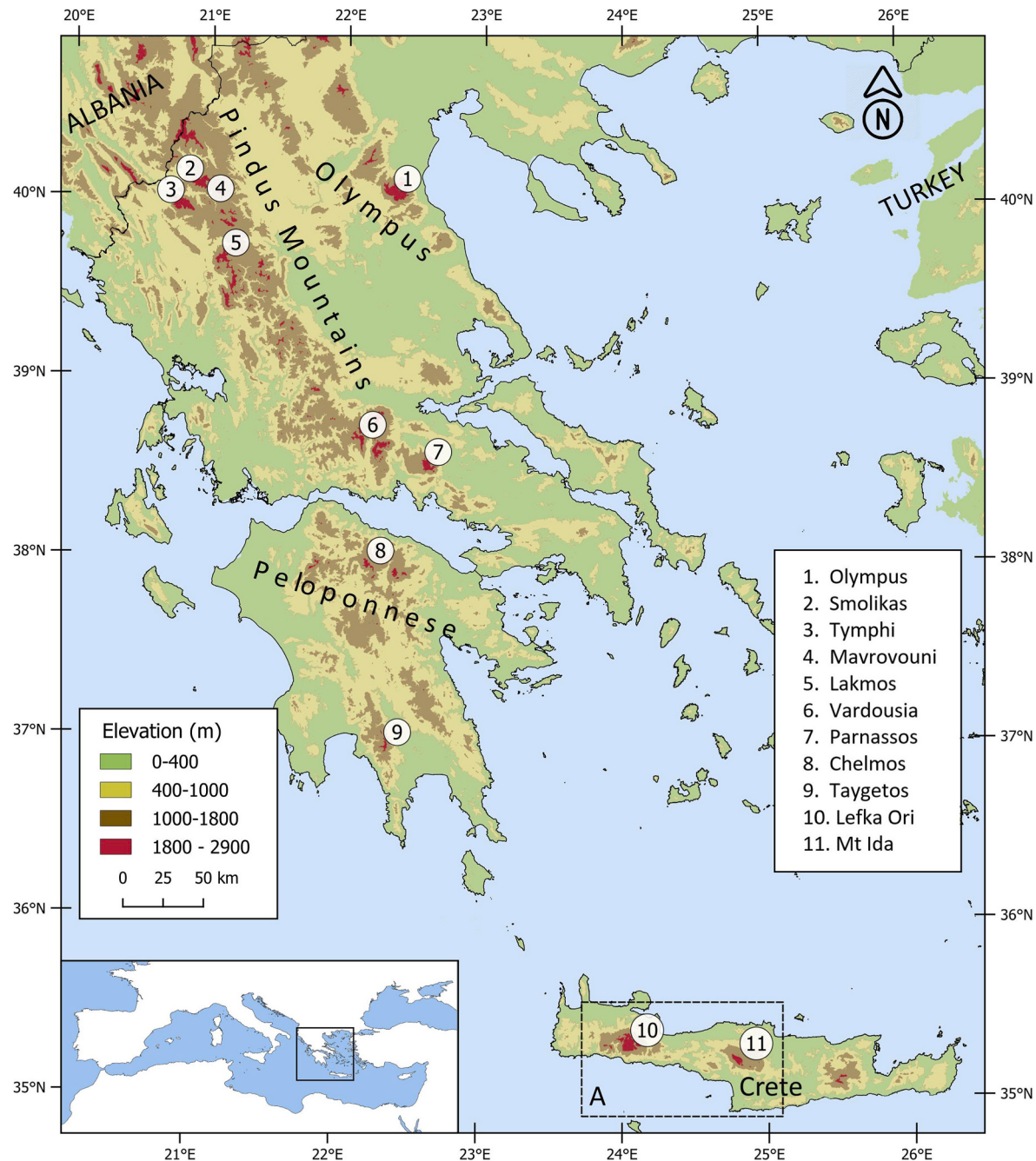


Fig. 1. The major mountain ranges of Greece with documented evidence of Quaternary glaciation. Panel A indicates the map extent shown in Fig. 3 (modified from Leontaritis et al., 2020).

et al., 2017; Styllas et al., 2018; Allard et al., 2020; Leontaritis et al., 2022). On Mt. Chelmos, the local Late Pleistocene glacial maximum occurred at $36.5 \pm 0.9 - 28.6 \pm 0.6$ ka, with a mean ELA of 2046 m a.s.l. (^{36}Cl ages; Pope et al., 2017; recalculated by Allard et al., 2020). However, glaciers on Mt. Tymphi and Mt. Mavrovouni reached their maximum extent near the global LGM. Glaciers on Mt. Tymphi had an ELA of 2016 m a.s.l., with terminal positions dating from $29 \pm 3.0 - 25.7 \pm 2.6$ ka (^{36}Cl dating; Allard et al., 2020), while on Mt. Mavrovouni, preliminary ^{36}Cl dating indicates a similar phase at 27.0 ± 6.5 ka and an ELA of 2090 m a.s.l. (Leontaritis et al., 2022). Geomorphological studies on Mt. Smolikas (Hughes et al., 2006b) and Mt. Olympus (Styllas et al., 2018) suggest that moraines at 2000–2200 m a.s.l. and 2155 m a.s.l., respectively, may correlate with a glacial advance phase synchronous to the LGM, though they lack numerical age constraints.

During the transitional phase from the LGM to the Late-glacial, glacial and periglacial evidence from Mt. Tymphi and Mt. Mavrovouni suggests cold, arid conditions unfavorable for glacier development, but cold and humid enough to preserve neve fields, permafrost, rock glaciers, and small glaciers in topographically favorable positions (Hughes et al., 2003; Allard et al., 2020; Leontaritis et al., 2022). Similar conditions are suggested on Mt. Chelmos by the presence of recessional moraines at $22.2 \pm 0.3 - 19.6 \pm 0.5$ ka (^{36}Cl ages; Pope et al., 2017; recalculated by Allard et al., 2020).

During the Late-glacial interval (17.5–11.7 ka; Rasmussen et al., 2006; Rasmussen et al., 2014) only marginal glaciers formed in high-elevation up-valley positions. Moraines have only been dated on Mt. Chelmos at $13.1 \pm 0.2 - 10.5 \pm 0.3$ ka (^{36}Cl ages; Pope et al., 2017; recalculated by Allard et al., 2020) and on Mt. Olympus at $13.0 \pm 0.5 - 11.7 \pm 0.5$ ka (^{36}Cl ages; Styllas et al., 2018; recalculated by Allard et al., 2020) at 2100 m a.s.l. and 2200 m a.s.l., respectively, indicating a glacial advance phase correlated with the Younger Dryas (12.9–11.7 ka; Rasmussen et al., 2014). Glacial deposits at 2300–2400 m a.s.l. on Mt. Smolikas were also linked to the Late-glacial upon stratigraphical position within a complete and well-preserved glacial sequence (Hughes et al., 2006b).

In the Holocene, Mt. Olympus is the only Greek mountain with evidence of glaciation, with small glaciers surviving in a high-elevation, 600m deep cirque, indicating strong local topoclimatic control (Styllas et al., 2018).

1.2. The Quaternary glacial record in Crete: comparisons with the southern Peloponnese

Before examining the potential glacial record in Crete, it is essential to first review the respective record in the nearest mountain range, where glacial deposits have been identified. Evidence suggests glaciers were present on Mt. Taygetos (2407 m a.s.l. - 1° south of Mt. Chelmos), located in the southernmost part of the Peloponnese and mainland

Greece (Fig. 1). Terminal moraines are found at 1850 m a.s.l. on the eastern slopes, while a large north-facing cirque contains deposits extending down to 1500 m a.s.l. (Maire, 1990a; Mastronuzzi et al., 1994). Kleman et al. (2016) revisited the geomorphology of Taygetos, noting a 'diagnostic imprint' left by glaciation during recent cycles. However, the geochronology and paleoclimatic significance of these features remain unexplored. Relatively extensive moraines in down-valley positions can be attributed to Middle Pleistocene glaciations, based on morphostratigraphic correlations with the glacial record in Greece. However, the presence of glaciers during the numerous stadials of the Last Glacial Cycle (MIS 5d-2) remains uncertain. Preliminary investigations of the NW cirques of Taygetos suggest the presence of moraines in stratigraphically younger, upvalley positions (Fig. 2). This may indicate glaciation during the LGM and Late-glacial periods, but this hypothesis requires testing through detailed geomorphological studies and absolute dating of the deposits.

The mountains of Crete lie just 1°40' south of Mt. Taygetos (Fig. 1) and reach similar elevations (Mt. Ida or Psiloritis at 2456 m a.s.l. and the Lefka Ori Mountains or White Mountains at 2453 m a.s.l.). Therefore, they likely bear traces of former glaciations, particularly of Middle Pleistocene phases. However, glaciation evidence in Crete has been contentious, necessitating further research and field observations from the highest parts of the mountains (Hughes and Woodward, 2009, 2017; Woodward and Hughes, 2011).

On Mt. Ida, early studies noted the absence of glacial deposits (Poser, 1957; Bonnefont, 1972), but Fabre and Maire (1983) reported the first glacial evidence, describing a well-preserved cirque-moraine system. However, their findings lacked photographs, location details, and topographic maps, leading to skepticism about the presence of a cirque on Mt. Ida (Woodward and Hughes, 2011). Maire (1990b) later confirmed the moraine with photographic evidence and a geomorphological map, though this book was not available digitally until March 2019, meaning it was overlooked in prior reviews (Woodward and Hughes, 2011; Leontaritis et al., 2020). Still, Hughes and Woodward (2017) suggested Mt. Ida probably holds the clearest glacial evidence. For Lefka Ori, several researchers (Poser, 1957; Bonnefont, 1972; Boenzi and Palmentola, 1982; Fabre and Maire, 1983; Maire, 1990b) found no glacial features. The Sphakia Survey, an archaeological investigation of the Lefka Ori region, also reported no evidence of glaciation in the region. Rackham and Moody (1996) noted that while glacial features were identified on Mt. Ida, they had not been confirmed on Lefka Ori. On the other hand, Hempel (1991) recognized 'fluvial-nival' deposits in both the Lefka Ori and Mt. Ida, linking them to Saalian glaciations based on U-series dating. Boenzi and Palmentola (1982) also noted evidence of nival processes in depressions close to the highest summit of Pachnes. Nemec and Postma (1993) argued that the alluvial fans on Lefka Ori's south piedmont were formed by large fluvial discharges related to ice cap wastage, suggesting the presence of cirque glaciers or an ice cap,

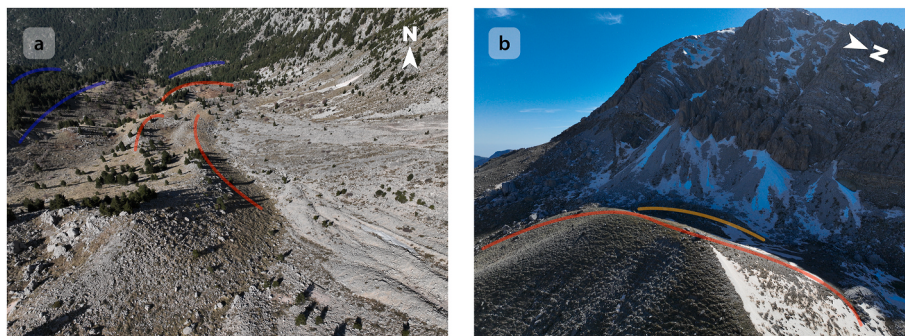


Fig. 2. a) Moraines in the NW cirque of Taygetos, where distinct stratigraphic units are visible. **b)** An upvalley, north-facing moraine and a pronival rampart below the Chalasmeno peak. Blue, red, and yellow lines represent different morphostratigraphic units, likely spanning from the Middle Pleistocene (blue) to the LGM (red) and even the Late-glacial (yellow). (UAV images: March 2024). (For interpretation of the references to colour in this figure legend, the reader is referred to the Web version of this article.)

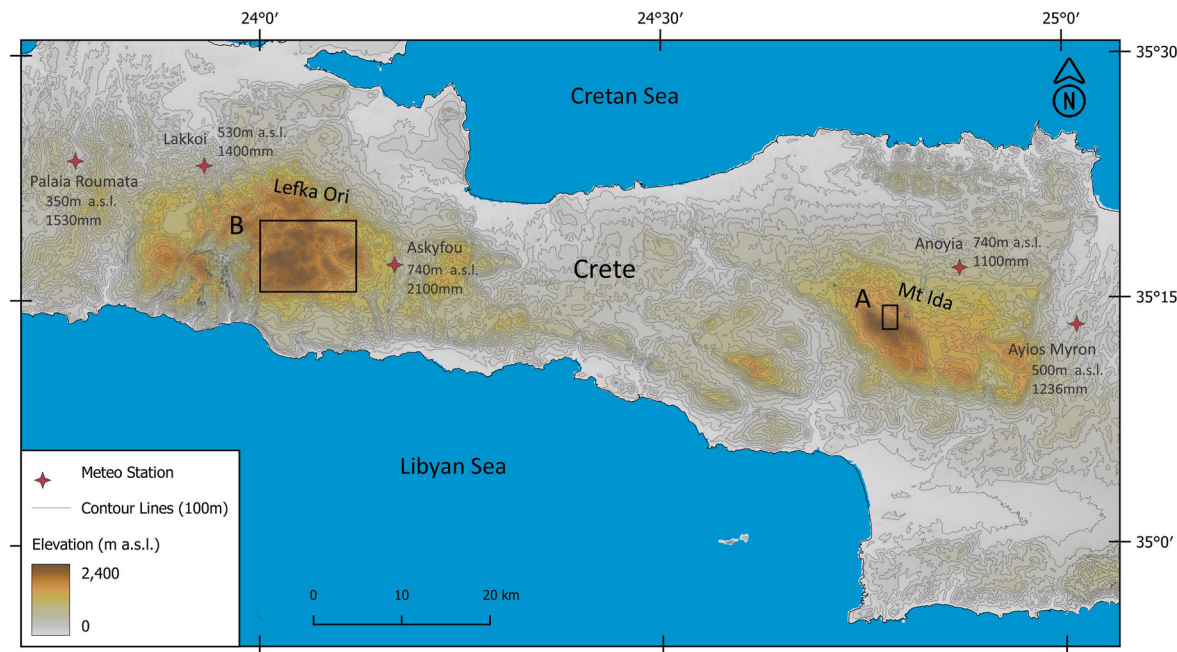


Fig. 3. Location map of the Lefka Ori and Ida massifs. Panels A and B correspond to the map extents depicted in Fig. 5 and 9, respectively. Precipitation data of meteorological stations from Gouvas and Sakellariou (2011) and Tzoraki et al. (2015).

though they provided no further evidence. These claims were criticized by Blair and McPherson (1995), and later studies revised the proposed cascading fan model as well as the derived links of sedimentation processes with the climate (Pope et al., 2008, 2016; Ferrier and Pope, 2012). Bathrellos et al. (2014, 2015) further confused the situation, claiming the presence of 5 cirques on Mt. Ida and 12 cirques in Lefka Ori covering 4.2 km² at an average elevation of 2186 m a.s.l.

1.3. Aims & objectives

This study revisits the mountains of Crete to address uncertainties surrounding their Quaternary glaciation history and associated paleoclimatic implications, with the aim of establishing a contemporary framework for interpreting Cretan glaciation within a broader regional paleoclimatic context. It integrates extensive field observations from Mt. Ida and the Lefka Ori with a critical review of existing geomorphological and sedimentary studies, taking into account the roles of paleoprecipitation, tectonic uplift, and topography in glacier development. The specific objectives were to identify and map glacial and periglacial landforms across substantial portions of the uplands of both massifs.

Fieldwork on Mt. Ida primarily focused on the cirque-moraine system initially described by Fabre and Maire (1983) and Maire (1990b) on the mountain's northern slopes, aiming to offer the first comprehensive reinterpretation of the Mt. Ida glacial sequence within a modern paleoglaciological framework by integrating contemporary analytical approaches with detailed field mapping. While earlier studies broadly attributed these deposits to a single Late Pleistocene (LGM/Würmian) glaciation, our analysis identifies multiple distinct Quaternary glacial phases and attempts to establish a preliminary relative chronological framework for glaciations based on correlations with the glacial record of mainland Greece. By placing these findings in the context of recent advances in Mediterranean paleoglaciology, this work provides new insights into the spatial and temporal variability of glaciation in southern Europe.

2. Regional setting

Crete is the southernmost of the major Mediterranean islands,

located at 35–36° latitude. It covers an area of 8305 km², with a length of 255 km, a width ranging from 13 to 45 km, and a coastline of 1056 km (Maire, 1990b). Situated in the forearc of the Hellenic subduction zone, Crete lies where the African Plate subducts beneath the Aegean microplate (Bonneau, 1984; McClusky et al., 2000; Petereck and Schwarze, 2004). Tectonically active since the Jurassic, Crete's crust consists of a nappe pile formed during mid-Cenozoic subduction and exhumed in the Late Cenozoic (Fassoulas et al., 1994; van Hinsbergen and Meulenkamp, 2006).

Crete's topography is dominated by high mountains and expansive massifs (Fig. 1). Among Greece's ten tallest peaks are Mt. Ida (also known as Psiloritis, 2456 m a.s.l.) located in central Crete, and the Lefka Ori Mountains (2453 m a.s.l.) in the west (Fig. 3). In contrast, eastern Crete features lower, yet widespread, mountains. Mt. Ida forms an elongated massif covering approximately 100 km² above 1000 m a.s.l., while Lefka Ori is a much more extensive massif, covering 385 km² above 1000 m a.s.l. and containing 40 km² and 30 peaks above 2000 m a.s.l. (Bergmeier, 2002; Vogiatzakis et al., 2003). Although a marked west-to-east precipitation decline characterizes the island, both the Lefka Ori and Mt. Ida receive significant amounts of precipitation as shown in Fig. 3. On Mt. Ida precipitation is in the range of 1000–1200 mm at 550–750 m a.s.l. and has been extrapolated to 1200–1400 mm at 1300–1500 m a.s.l. and to 1500–1800 mm at 1700–2200 m a.s.l. (Maire, 1990b; Climatic Atlas of Greece, 2020). The Lefka Ori are even wetter, with precipitation exceeding 2100 mm at 750 m a.s.l. in the east and ranging from 1400 to 1500 mm at 350–530 m a.s.l. in the northwest (Fig. 3). Precipitation is therefore extrapolated to 2200 mm above 1500 m a.s.l. and could reach over 2500 mm in the summit plateau above 2000 m a.s.l. (Maire, 1990b; Climatic Atlas of Greece, 2020), exceeding precipitation in the Pindus mountains in the much wetter northwestern Greece (Gouvas and Sakellariou, 2011; Leontaritis et al., 2022). Thus, the climate in the mountains of Crete resembles that of massifs in mainland Greece, particularly the Peloponnese, with a wetter western side and a drier eastern side, and higher summer aridity than northern Greece (Maire, 1990b). Significant snowfall occurs every winter in these high mountains. However, there are no glaciers, permafrost, or permanent snowfields today. Snow cover on the northern slopes above 1800 m a.s.l. persists from early December to late May.

The summit areas of both massifs are predominantly composed of limestones, dolomites, and marbles of the para-autochthonous ‘Plattenkalk’ series, representing distinct lithological units of varying origins and ages (Jacobshagen, 1986). Its upper 1000 m, primarily exposed on the summit of Mt. Ida and the western sector of the Lefka Ori, comprise platy, thin-bedded crystalline limestones dating from the Upper Jurassic to the Eocene. On the contrary, the central highlands of the Lefka Ori are dominated by the lowest unit of the Plattenkalk series (Moraetis et al., 2024, 2025). The upper section of this unit consists of Triassic to Liassic massive white and grey limestones and marbles, while the lower section comprises medium-bedded to massive grey, and black dolomites and stromatolites that alternate both laterally and vertically. This zone is characterized by very intense karstification. Sinkhole/doline fields are found at various altitudes between 1600 and 2100 m a.s.l., developed directly within carbonate rocks both in the barren landscape and in the underground karst systems. Over 1400 sinkholes and caves have been mapped in the central Lefka Ori massif, such as the Gourgouthakas cave (1208 m deep), the Lion cave chasm (1110 m deep), and the Sternes cave (595 m deep) (Adamopoulos, 2005, 2013; Zacharias et al., 2022).

3. Methods

Geomorphological mapping followed the principles in Chandler et al. (2018) for alpine environments, incorporating remote sensing and field data. Reconnaissance analysis was built on previous studies (Lefka Ori, Mt. Ida in Maire, 1990b) using topographic maps (e.g., Anavasi, 2023, 2024; Open Street Maps), regional geological sheets of the Greek Institute for Geological and Mineral Exploration (Bonneau et al., 1984; Katsivrias et al., 2008), and satellite imagery (Google Earth, Bing Maps). Additionally, UAV-captured aerial photos and panoramic images from the Psiloritis UNESCO Global Geopark (<https://tours.panotours.gr/Ida/>) were key for mapping and interpreting the Migero cirque/moraine system. The Digital Elevation Model (5 m resolution) was provided by the National Cadastre SA. Field validation of the reconnaissance sketch-map and the available geological/geomorphological maps were performed alongside mapping with a GPS/Glonass device (Garmin 64s) during multiple field trips between 2022 and 2024. The digital mapping and the creation of maps were conducted in the open source QGIS environment. The cross-section and longitudinal profiles were extracted using the profile tool in Qgis. Glacial features were classified based on morphostratigraphic criteria, such as relative stratigraphic position, elevation, sediment composition (e.g. clasts size and shape, presence of fines), and evidence of exhumation, following Hughes (2010).

3.1. Glacier reconstructions and ELA calculations

Paleoglaciers on Mt. Ida were reconstructed using a Geographic Information System (GIS)-based workflow implemented in the Palaeoice toolbox (Li, 2023). This semi-automated tool extends the numerical approach of Benn and Hulton (2010) and Pellittero et al. (2016), incorporating substantial methodological enhancements by Li (2023). Glacier geometry was modeled from automatically derived shear-stress values and shape factors along flowlines, with ice-surface elevation rasters and glacier outlines generated using the “fit” method of Li et al. (2012). Glacier limits were delineated primarily from geomorphological field evidence, including terminal and lateral moraines. Where evidence was incomplete or absent, glacier boundaries were inferred from the typical morphology and rheology of valley glaciers. Equilibrium-line altitudes (ELAs) were calculated automatically using the area-altitude balance ratio (AABR) method (Osmaston, 2005) that incorporates both glacier hypsometry and mass-balance gradients. This was implemented in the GIS tool of Pellittero et al. (2015) with a balance ratio of 1.56, the mean value for present-day glaciers in comparable Mediterranean mountain ranges (Rea, 2009).

4. Results & interpretation

4.1. Mt. Ida (Psiloritis)

It is noteworthy that the reconnaissance study of satellite imagery on the uplands of Mt. Ida did not indicate any glacial landforms beyond the Migero plateau (Fig. 4). This observation is consistent with the findings of Fabre and Maire (1983) and Maire (1990b). Still, we conducted a field survey in the entire high-elevation zone (>1700 m a.s.l.) of the massif without finding any additional evidence of glaciation.

4.1.1. The Migero cirque/moraine system

The moraines above the Migero plateau constitute a prominent glacial feature. These moraines are identifiable in commercial satellite imagery (e.g., Google Earth, Bing Maps) along the northern slopes, just below the massif's highest peak, and correspond to the geomorphological sketch map presented in Maire (1990b). The field survey confirmed the presence of this Quaternary cirque-moraine system. While the detailed geomorphological description provided by Maire (1990b) is partially adopted here, the deposits are interpreted as part of a complex glacial sequence rather than as deposits from a distinct glacial phase (Fig. 4).

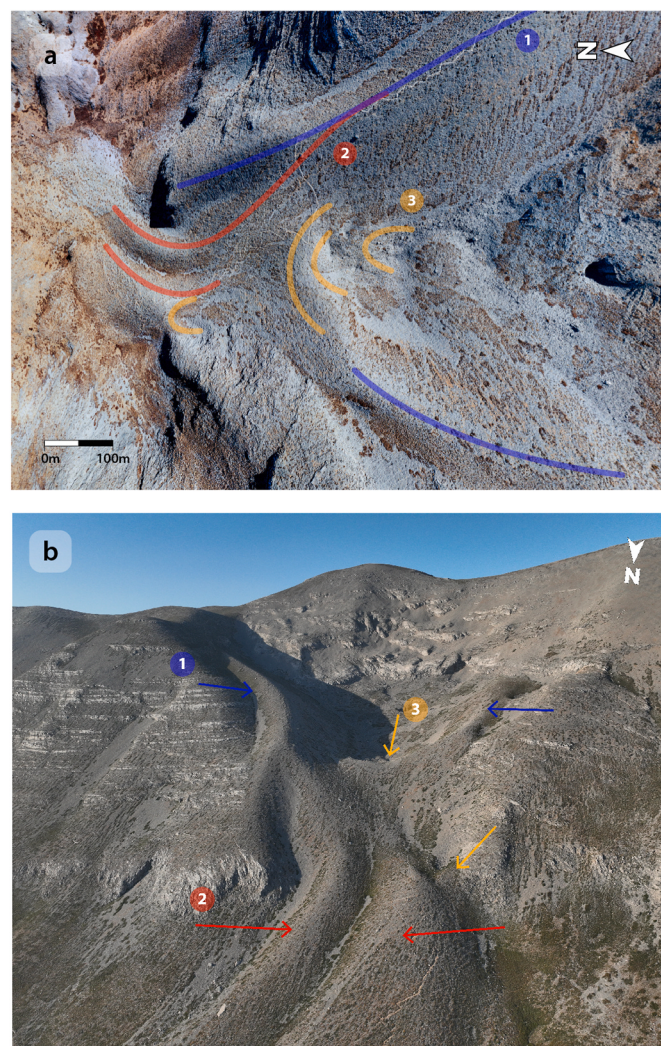


Fig. 4. a) Mosaic of aerial photographs showcasing the Migero cirque-moraine system (source: <https://tours.panotours.gr/Ida/>) b) Aerial photograph of the Migero moraines (July 2024). Blue, red, and yellow lines represent Units 1, 2, and 3, respectively. (For interpretation of the references to colour in this figure legend, the reader is referred to the Web version of this article.)

The 800-m-wide Migero cirque is well-formed, extending from approximately 2300 to 2000 m a.s.l. and oriented to the north. Its walls and slopes are steep, ranging locally from 60 to 65° in the upper sections to 35–40° in the lower parts. The morphology of these slopes results from the intersection of two normal faults, oriented E-W and NW-SE (Fassoulas, 1999, 2001), which define both the northern escarpment of Mt. Ida and the tectonic amphitheater within which the cirque has evolved (Fig. 4b). No glacial deposits were identified in the slopes adjacent to the Migeros cirque, despite having similar orientation and position below the ridgeline and are also characterized by cirques at their headwalls.

Lithology consists of Jurassic to Eocene thin-bedded marble with silica intercalations from the Plattenkalk series, with some levels displaying intense folding (Fassoulas et al., 2004). The cirque walls are characterized by ice-polished bedrock, which is surprisingly well-preserved given the erosion-prone calcareous lithology. Nonetheless, run-off karstification channels (rillenkarren) are evident on these ice-moulded surfaces. Rain and snowmelt infiltrate through the karstic system, with no evidence of surface run-off streams. A talus cone, composed of angular debris from the cirque walls, forms the lower part of the slope. These scree deposits extend down to the glacio-karst depression, partially covering the glacial deposits on the valley floor.

A glacial geomorphological map of this cirque-moraine system is presented in Fig. 5. The mapped moraines are classified into three distinct sedimentary units (1–3) based on the morphostratigraphic observations described below. It is here noted that, although distinct, Unit 1 and Unit 2 were not necessarily formed during separate glacial periods; instead, they may correspond to different glacial phases within the same cold stage.

The deposits of Unit 1 and 2 are primarily represented by typical lateral moraines characterized by sub-rounded to sub-angular clasts and boulders, along with ample amounts of unsorted gravels and sands (Fig. 6a-c). While these moraines are generally well-preserved, signs of extensive degradation and erosion are evident in some areas. The lateral moraines of Unit 1 are stratigraphically distinct from the lateral and terminolateral moraines of Unit 2, as indicated by the differences in their morphology described next. The eastern moraine crest is split into two distinct sections, which appear to have formed independently (Figs. 4, 5 and 7a). The outer crest corresponds to a larger and wider glacier with indistinct down-valley depositional limits (Unit 1), whereas the stratigraphically younger Unit 2 moraine merges with the western moraine and extends down to approximately 1730 m a.s.l., forming a glacial tongue that transitions into a glaciofluvial fan (Figs. 4, 5, 6d and 7a). The sediments/deposits of this fan share the same characteristics as the

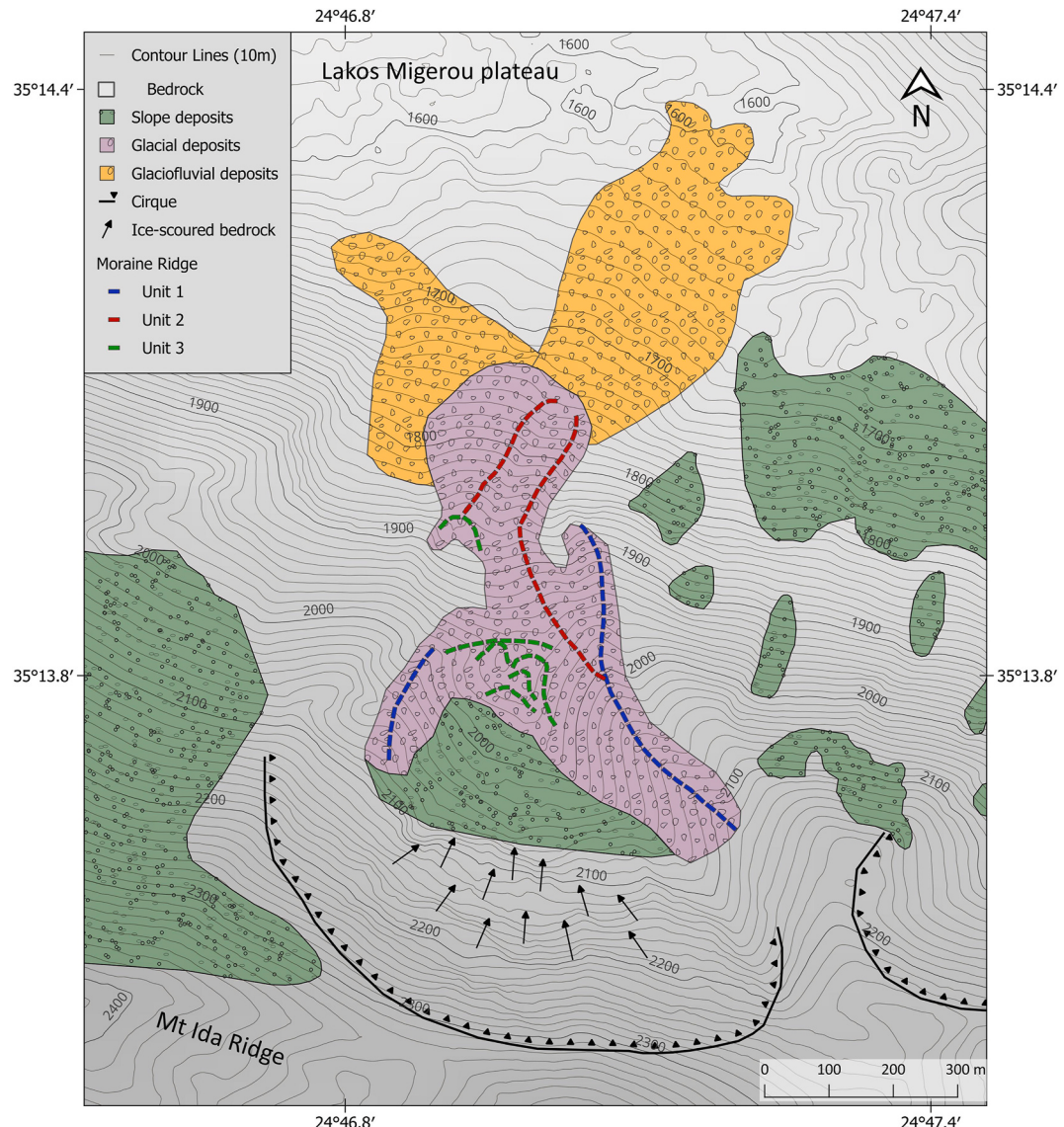


Fig. 5. Glacial geomorphological map of the Migero cirque-moraine system (Panel A in Fig. 3).



Fig. 6. a-c) Unit 1/2 deposits characterized by fine materials (gravels and sands) interspersed with subrounded boulders and clasts; d) Glaciofluvial deposits extending down to 1600 m a.s.l. within the Migeros Polje.

glacial deposits of Unit 1 and 2, with some larger, rounded boulders scattered throughout, filling the eastern part of the Migero polje (Fig. 6d).

Distinguishing between Units 1 and 2 along the western lateral moraine is challenging. The mid-section has been eroded and partially overridden by a younger glacier or ice field, classified in Unit 3. This interpretation is supported by the overlapping features visible in Figs. 4 & 7a-b. However, the lower part of the western moraine, associated with Unit 2, is notably wider than the eastern branch (Fig. 4), suggesting it may comprise deposits from both Unit 1 and Unit 2, merged during glacial activity.

The prominent terminal moraine at approximately 1940 m a.s.l. is morphostratigraphically distinct from the higher-elevation lateral moraines of Unit 1 and 2 and the terminolateral moraines of Unit 2 below it, as it is clearly nested within the older moraines (Fig. 7a-b). Similarly, another terminal moraine is nested slightly lower within the western branch of Unit 1 and 2 deposits. Both moraines are therefore attributed to the stratigraphically younger Unit 3.

Upvalley, hummocky moraines and glacially transported sediments with indistinct depositional limits are also attributed to Unit 3 (Fig. 4). These features likely correspond to a glacial retreat phase, forming recessional moraines, or an oscillation phase characterized by multiple advances, standstills, and retreats. This unit of glacial deposits appears to have been formed by small glaciers with a substantial debris load.

In comparison to Unit 1 and 2, the deposits of Unit 3 are noticeably more angular, contain fewer fines, and appear to be less exhumed and eroded (Fig. 6 a-c and 7c-d). These deposits are further distinguished by the presence of several large boulders that are significantly less eroded and rounded than those found in Unit 1 and 2, implying a much younger depositional age for Unit 3. Similar depositional configurations have been documented on Mt. Tymphi, Mt. Olympus, Mt. Mavrovouni, and Mt. Chelmos (see Introduction for references). A supraglacial or névé field origin is unlikely, as this landform does not exhibit the typical characteristics of pronival ramparts (Hedding and Sumner, 2013; Matthews et al., 2017 and references therein).

4.1.2. Glacial reconstructions and ELAs on Mt. Ida

The ELA of paleoglaciers can be estimated based on the maximum elevation of well-preserved, undegraded lateral moraines, as ice flow lines typically converge toward the glacier center above the ELA and

diverge toward the margins below it (Nesje, 1992; Bakke and Nesje, 2011). In this context, the ELA of the glaciers that formed Unit 1 moraines is estimated to be approximately 2120 m a.s.l. In order to elaborate this further, the paleoglaciers of the three glacial phases were reconstructed using the *Palaeoice* toolbox (Li, 2023) and the respective ELAs were calculated with the altitude balance ratio (AABR) method using the GIS tool of Pellitero et al. (2015). The results of these calculations are summarized in Table 1 whereas a graphical representation of the reconstructed paleoglaciers during these three phases is presented in Fig. 8.

4.2. The Lefka Ori mountains

The high-elevation zone (>1800 m a.s.l.) of Lefka Ori, where glacial features are most likely to be found, spans over 120 km² (Fig. 9). This area includes more than 30 peaks exceeding 2000 m a.s.l., 15 of which rise above 2200 m a.s.l. (Maire, 1990b; Bergmeier, 2002; Vogiatzakis et al., 2003). However, a preliminary analysis of satellite imagery did not reveal any evidence of glacial features, leading to the prioritization of field mapping in areas below the massif's highest peaks (>2200 m a.s.l.).

The uplands of Lefka Ori are characterized by two primary lithological zones within the Plattenkalk Formation (see section 2). These lithologies exhibit distinct erosion patterns and differences in sediment deposition and preservation (Fig. 10). Consequently, the fieldwork strategy aimed to encompass a diverse range of representative environments for each lithological zone (Fig. 9). These included valleys, cirques, plateaus, fans, and sediment traps within karstic depressions.

No clear glacial or periglacial features were identified. Field verification did not confirm the cirques previously mapped by Bathrellos et al. (2014, 2015) from satellite imagery; instead, those features are more likely hollows produced by combined karstic and tectonic processes. Therefore, this section focuses on features potentially linked to past glacial activity: (i) the prominent U-shaped valleys in the southern part of the massif and (ii) several boulder-rich alluvial fans situated below high-elevation, north-facing slopes in the northeastern sector (Mikros Trocharis area).

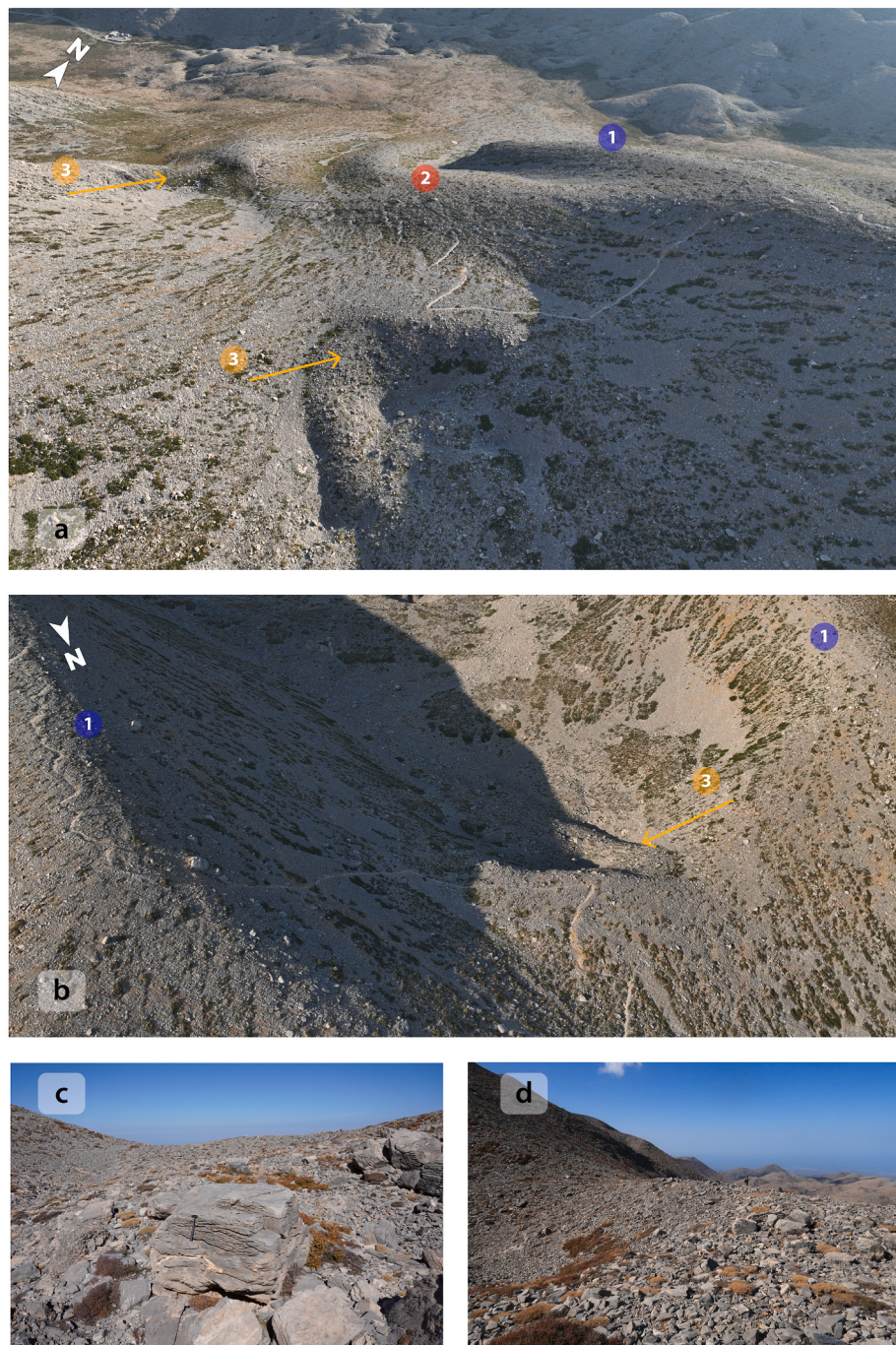


Fig. 7. a-b) Stratigraphic distinction of the two younger moraines (Unit 3) nested within the Unit 1 and 2 deposits; c-d) Details of the Unit 3 deposits denoted above. These deposits are less exhumed, sub-angular, and contain fewer fine materials (gravels and sands) compared to Unit 1 and 2.

4.2.1. U-shaped valleys in southern Lefka Ori (Ammoutsera and Mavri Laki)

The black dolomite area in the southcentral part of the massif is characterized by wide almost U-shaped valleys with eroded slopes resembling ice-polished surfaces (Fig. 11a), which have likely led previous researchers to attribute their formation to large valley glaciers (see Introduction). These valleys originate at altitudes greater than 2200 m a.s.l. and terminate at 1800 m a.s.l. on the western slopes and 1500 m a.s.l. on the southern slopes. A detailed field survey was conducted in the Ammountsera Valley, while the Mavri Laki Valley was examined through a UAV survey.

In the Ammountsera Valley, lithified unsorted deposits were observed within karstic hollows. Caution is warranted to avoid misinterpretation

of these deposits as tillite (Fig. 11b). The rock comprises semi-rounded clasts—ranging from sands and gravels to rocks and boulders—derived from the surrounding lithologies and cemented by calcareous material. These deposits are scattered throughout the valley, primarily within karstic depressions, and are also found on slopes high above the valley, ruling out in-situ glacial deposition. Maire (1990b) attributed their formation to the Early Miocene, filling inherited karst hollows. However, it is also plausible that these deposits correspond to what is described in the IGME (Institute of Geology and Mineral Exploration) geological map as ‘synsedimentary brecciated carbonate horizons with carbonate cement and voids filled locally with clayey material’ (Vidakis et al., 1993), which are part of the Upper Triassic bedrock formations.

Table 1

Glacier reconstructions associated with defined morphostratigraphic units on Mt. Ida.

Sedimentary Unit	Max. Thickness (m)	Length (m)	Area (km^2)	ELA ^a
1	68.9	1490	0.72	2073 m a.s.l.
2	73.4	1220	0.38	2087 m a.s.l.
3	58.7	750	0.28	2101 m a.s.l.

^a Calculated with the AABR method using a Balance Ratio of 1.56 (see section 3.1).

The prominent open U-shaped valleys in southern Lefka Ori were likely not formed by extensive valley glaciation, as evidenced by the absence of characteristic glacial or periglacial features. Instead, their origin appears to be polygenetic, with karstification playing a dominant role. Analysis of valley cross-sectional profiles (Fig. 12a) shows that they can be approximated by a parabolic function ($y = ax^b$), with the fits yielding high R^2 values. Although the exponent coefficient b falls within the range of 1.5 to 2—typical of glacial U-shaped valleys (Evans, 2007)—this metric has been shown to be only partially reliable for determining glacial origin (Zimmer and Gabet, 2018). For comparison, Fig. 12b presents cross sections of typical glacial U-shaped valleys in British Columbia. Furthermore, although both open U-shaped and glacial valleys can be modeled using quadratic equations ($y = a + bx + cx^2$), the coefficient c has been shown to be an entirely unreliable indicator for determining glacial origin (Zimmer and Gabet, 2018). Lithology exerts significant control on valley cross-sectional morphology (Zimmer and Gabet, 2018; Augustinus, 1992, 1995). Rock strength and the density of mechanical discontinuities influence valley form by promoting broader profiles in weaker lithologies and narrower forms in more resistant rocks (Bernard et al., 2021). Despite this, morphometric data for U-shaped valleys developed in limestone remain limited, and the role of post-glacial erosion in shaping the current profiles is still poorly understood.

Examination of the longitudinal profiles of the open U-shaped valleys in Lefka Ori (Fig. 12c) reveals that, unlike typical glacial valleys, which generally exhibit continuous downslope gradients and open drainage (Evans, 2007), the Lefka Ori valleys are characterized by blind sections that terminate in extensive karstic fields marked by sinkholes and dolines. These features are indicative of an endorheic drainage system of

karstic origin, as also suggested by hydrological studies in the area (Stamati et al., 2006; Lilli et al., 2020), and further emphasize the predominant role of karstification in the formation and evolution of these valleys.

4.2.2. Alluvial fans in northeastern Lefka Ori (Mikros Trocharis area)

Mikros Trocharis is a peak in the northeastern part of the massif, reaching an elevation of 2150 m a.s.l. Its main ridge spans approximately 3 km and extends between 2150 and 2000 m a.s.l. along an east–west axis. Lithologically, Mikros Trocharis is dominated by the Upper Triassic to Lias white recrystallized limestones, overlying black dolomites (Fig. 13). The northern slopes of Mikros Trocharis are relatively steep (30–50°) but transition into narrow shelves at lower elevations (1650–1450 m a.s.l.). These shelves host several fans and sediment traps within the intensely karstified black dolomites.

The westernmost fan, designated as Fan A in Fig. 13, is located near the entrance of the Lion Cave (1100 m deep) at an elevation of 1650 m a.s.l. This fan occupies a depression among black dolomites and grey limestones and is rich in fine sediments, including gravels, sands, and silt (Fig. 14a). Interspersed throughout are sub-rounded clasts of varying sizes, including boulders exceeding 2 m in diameter (Fig. 14a–b). The sediment composition reflects a mixture of the surrounding lithologies, incorporating clasts of lithified angular debris likely derived from the erosion of the overlying slopes. The lower slopes in some areas are overlain by a meter-thick layer of lithified angular colluvial deposits devoid of fine material. Elsewhere, these slopes are primarily covered with loose angular debris originating from the white limestones and marbles at higher elevations. Additionally, large black dolomite boulders were found resting on grey limestone below the black dolomite zone, near the entrance of Gourgouthakas Cave (1208 m deep Fig. 13) at an elevation of 1550 m a.s.l. (Fig. 14c). This evidence suggests high-energy transportation and deposition processes, but there is no evidence indicating a glacial origin.

To the east of Fan A, two similar fans (Fans B and C, Fig. 13) were identified at an elevation of approximately 1400 m a.s.l. Unlike Fan A, both fans are located below cirque-like indentations on the source slope. Fan B is composed of unsorted sediments of varied lithology, with indistinct depositional boundaries. A notable feature of Fan B is the presence of large, sub-rounded white marble boulders resting on the black dolomites. In some locations, these boulders have been deposited on small elevations near the fan (Fig. 15a). The most likely origin of these boulders is gravitational deposition through rockfalls, a process commonly observed elsewhere in Lefka Ori. They should therefore not

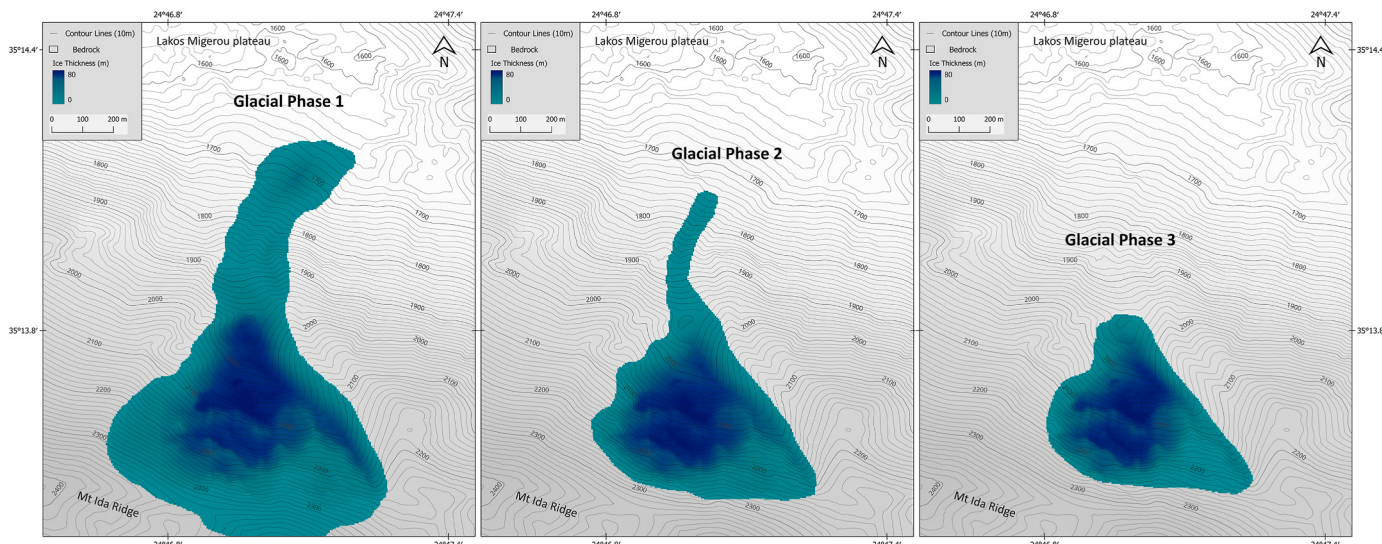


Fig. 8. Reconstructed paleoglaciers during three distinct glacial phases, corresponding to the identified sedimentary units.

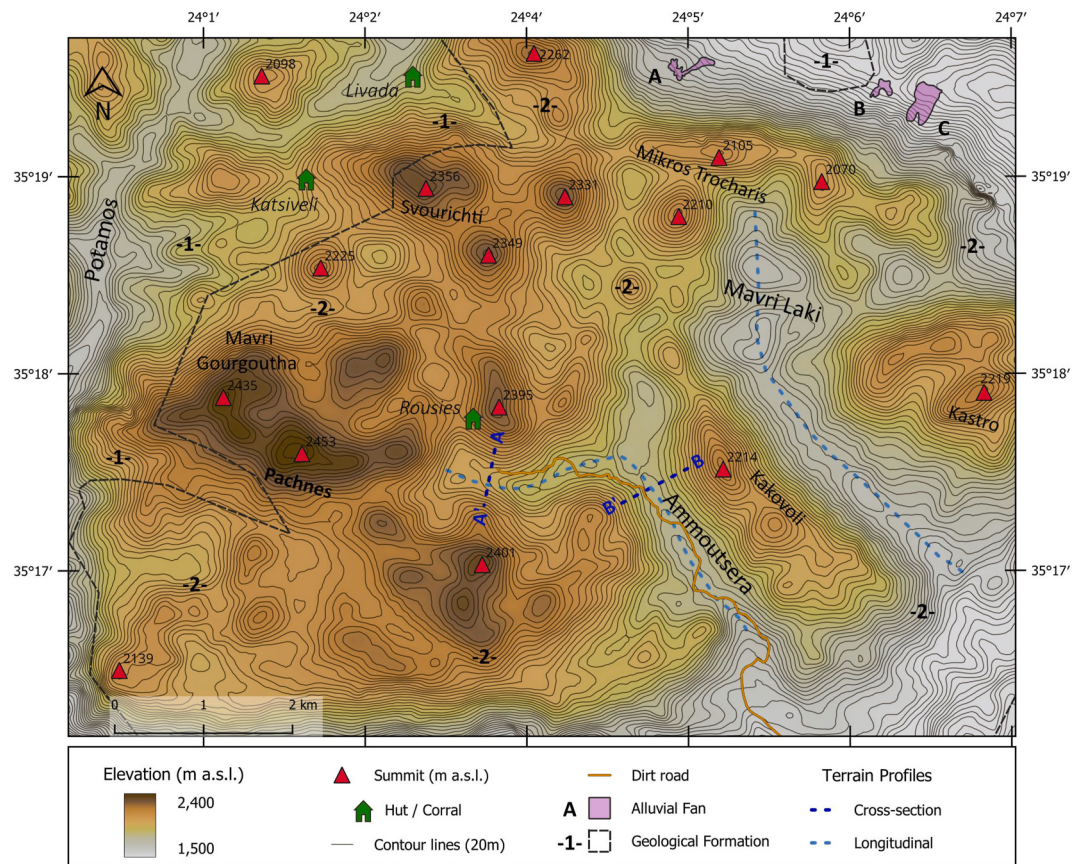


Fig. 9. Topographic map of the study area within the Lefka Ori massif, corresponding to Panel B in Fig. 3. Geological formations according to Moraetis et al. (2025) (see section 2 for detailed descriptions). The annotated polygons, labeled A to C, denote the alluvial fans discussed in the text. Terrain profiles refer to Fig. 12.

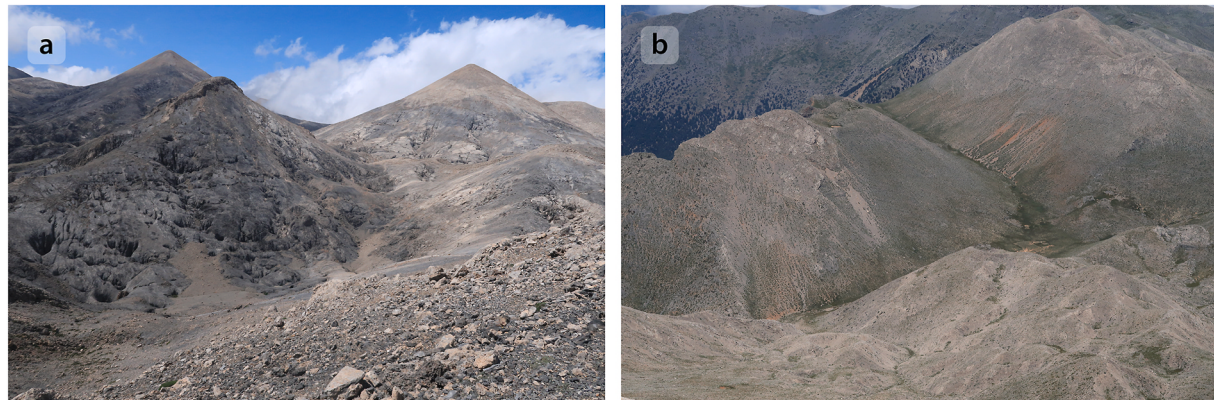


Fig. 10. Erosion patterns across different lithologies: **a**) Intensively karstified Triassic black-to-white dolomites, overlain by younger Triassic white marbles, dominate much of the central uplands of Lefka Ori (Formation 2 in Fig. 9); **b**) Thin-bedded Eocene limestones cover most of the western part of the massif (Formation 1 in Fig. 9).

be interpreted as glacially transported erratics. The sub-rounded shape of the boulders can be attributed to post-depositional weathering and, in some cases, fluvial erosion. Similarly, Fan C contains large sub-rounded boulders embedded within the fan. These boulders could have originated from rockfalls, but they could also have been transported from higher elevations by high-energy fluvial processes (Fig. 15b).

The characteristics of the fans described here differ markedly from the high-elevation alluvial fans found in depressions elsewhere within the uplands of the Lefka Ori mountains. The latter are typically composed of semi-sorted, finer, and more angular sediments (Fig. 15c),

suggesting a different depositional process compared to the Mikros Trocharis fans. Additionally, these high-elevation fans generally lack larger boulders, except in cases where such boulders have clearly detached from nearby cliffs or slopes (Fig. 15d).

Overall, the observations presented in this section suggest that the Mikros Trocharis fans are of high-energy fluvial origin, characterized by the presence of large boulders likely resulting from rockfalls. Notably, the absence of typical glacial deposits, such as moraines or tillite, coupled with the relatively low elevation of the Mikros Trocharis ridge, renders a glacial origin for these fans highly unlikely.

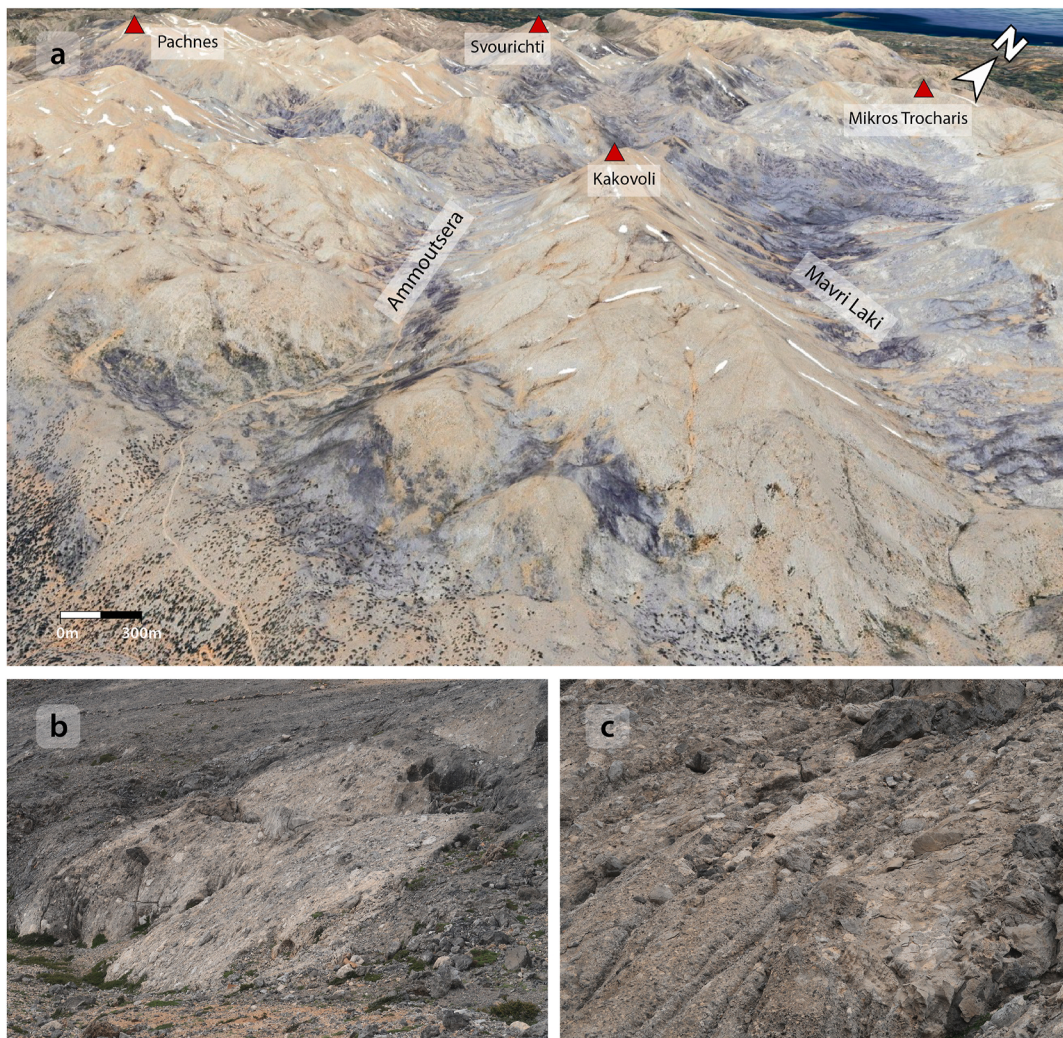


Fig. 11. a) Google Earth view of the Ammoutsera and Mavri Laki valleys draining the southern part of Lefka Ori. No evidence supporting glacial origin has been identified in these valleys; b) Lithified unsorted deposits in the Ammoutsera valley, potentially misinterpreted as tillite. The right picture highlights rillenkarren features formed by surface weathering of the rock.

5. Discussion

5.1. Relative chronology of Quaternary glacial phases on Mt. Ida

The sequence of glacial deposits on Mt. Ida can be correlated with the glacial record of mainland Greece. The nearest dated moraine sequence is on Mount Chelmos in the Peloponnese (340 km distance, 2.6° further north) where at least three distinct phases of glaciation have been identified using cosmogenic exposure and U-series dating (see Introduction). The oldest and most extensive glacial deposits date to the Middle Pleistocene, whereas ice extent was significantly smaller during the Last Glacial Cycle and the LGM. The glacial sequence on Mount Chelmos is the same as on Mount Tymphi in NW Greece 250 km distance and a further 2° further north. In fact, the glacial sequence is replicated up the western Balkans with the glacial sequence almost identical in character from the Peloponnese to Montenegro (Hughes et al., 2010, 2011) and indeed to the Croatian Dinarides (Marjanac, 2012). Thus, it seems a reasonable assumption to extrapolate southwards of this glacial sequence to Crete. However, eastward extrapolations of the Dinaric–Pindus glacial sequence are less reliable, as Late Pleistocene glaciations are known to have been more extensive east of the Dinaric–Pindus range, particularly in Turkey (Akçar et al., 2017; Sarıkaya and Çiner, 2017). Typically, from Croatia to Greece, Middle Pleistocene deposits are much more extensive and eroded, while younger deposits tend to be

more well-preserved and are confined to topographically favorable, up-valley positions (Leontaritis et al., 2020). On Mt Ida, the moraines of Unit 1 and Unit 2 exhibit characteristics similar to the Middle Pleistocene (MIS 12 & MIS 6) deposits found on Mt Tymphi (Hughes et al., 2006a; Allard et al., 2020), Mt Mavrovouni (Leontaritis et al., 2022) and Mt Chelmos (Pope et al., 2017, 2023), with significantly greater extent as well as erosion and dismantling compared to the stratigraphically younger, Late-Pleistocene deposits. Consequently, these moraines can tentatively be attributed to the Middle Pleistocene. However, assigning them to distinct glacial phases, such as MIS 12 and MIS 6, remains speculative, as the deposits of Unit 1 and Unit 2 could represent glacial advance and retreat phases within the same cold stage.

In contrast, the younger deposits of Unit 3 are notably less eroded, with fewer fines and more angular clasts. These features suggest a correlation with the Late Pleistocene glacial phase in mainland Greece, approximately coinciding with the LGM (Allard et al., 2020; Pope et al., 2017, 2023; Leontaritis et al., 2020, 2022). It is noteworthy that, although the glacial sequence in Mt. Ida shares commonalities with mainland Greece, the Middle Pleistocene glacial extent is significantly smaller. This indicates less favorable conditions for glacier development and insufficient ice accumulation for the formation of ice caps, consistent with a warmer climate associated with a 2.5°–4.5° latitude difference compared to the massifs of mainland Greece (Fig. 1). Thus, although correlations with mainland Greece are relevant, significant

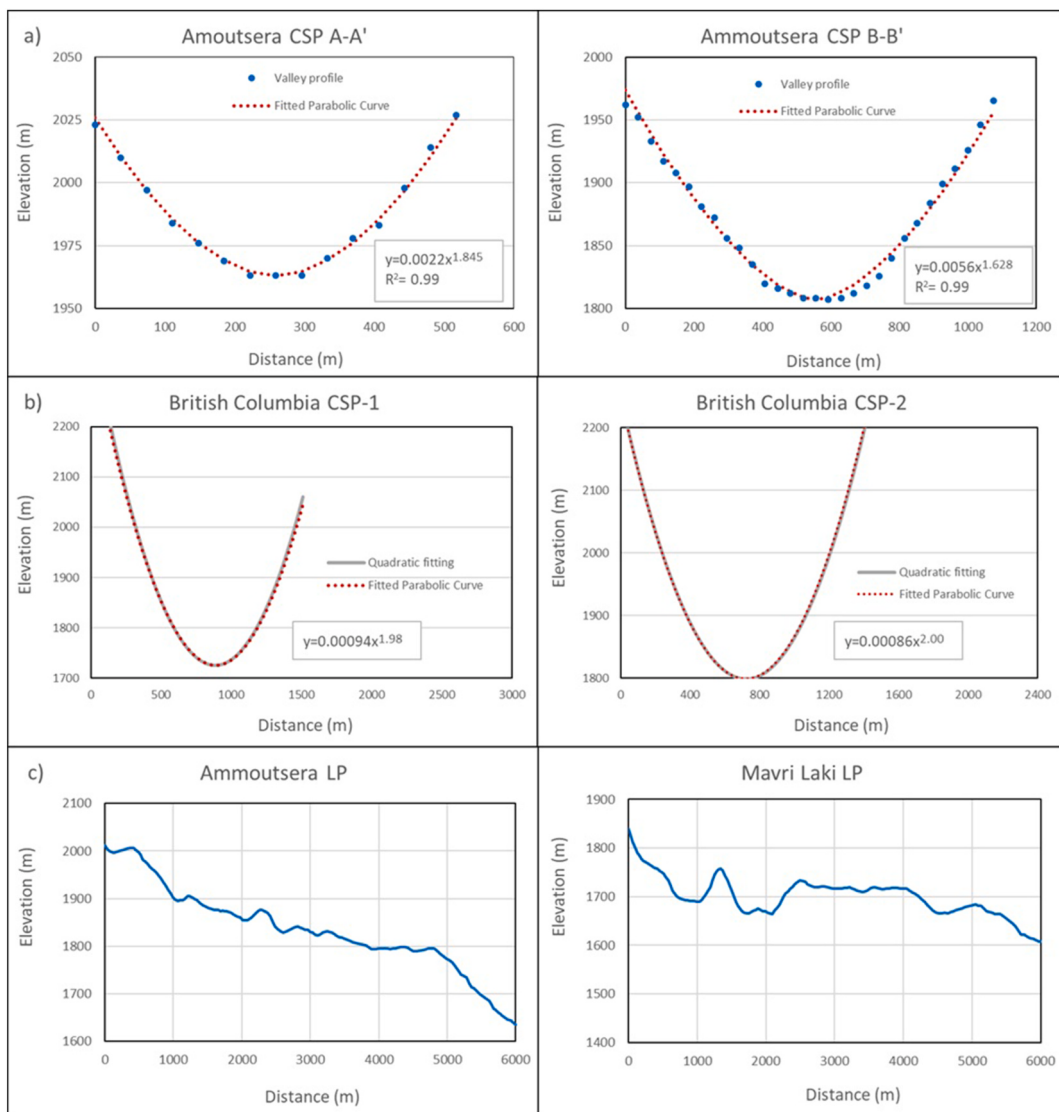


Fig. 12. a) Representative cross-section profiles of open U-shaped valleys in Lefka Ori and fitted parabolic curves; b) Quadratic fitting curves to CSPs of typical glacial U-shaped valleys in British Columbia ($R^2 \approx 0.973$; modified from Evans, 2007) and fitted parabolic curves; c) Longitudinal profiles (LP) along the Thalwegs of the main Ammoussera valley (left) and the Mavri Laki valley (right). The location of these profiles is shown in Fig. 9. CSP and LP profiles are plotted with Y:X axis ratios of 1:6 and 5:6, respectively, to maintain a consistent aspect ratio.

differences specific to Crete must also be considered. Importantly, these tentative chronological correlations remain hypotheses that require validation through absolute dating techniques in future research.

5.1.1. Absolute dating challenges

The absolute dating of the different glacial phases on Mt. Ida is a necessary step toward fully exploring its paleoclimatic significance. The following section discusses various aspects of dating the glacial deposits in the Migeros area.

The most widely used technique for dating glacial deposits is cosmogenic surface exposure dating of glacial boulders. The only cosmogenic nuclide suitable for limestone lithologies is ^{36}Cl (Alfimov and Ivy-Ochs, 2009). Additionally, numerous glacial boulders greater than 1.5 m in diameter, located along the moraines within the Migeros cirque on Mt. Ida, are well-suited for ^{36}Cl surface exposure dating. This technique has been demonstrated to reliably date Late Pleistocene moraines in the mountains of Greece, particularly those formed within the past 40 ka in Greece (e.g. Pope et al., 2017; Styllas et al., 2018; Allard et al., 2020). For example, in the Pindus Mountains, age control of Late

Pleistocene moraines using ^{36}Cl surface exposure dating on limestones (Mt. Tymphi, Allard et al., 2020) and ophiolites (Mt. Mavrovouni, Leontaritis et al., 2022) yielded consistent results. These studies placed the local LGM glacial maximum within a close time frame, well within age uncertainties ($25.7\text{--}29.0 \pm 3.0$ ka vs. 27.0 ± 6.5 ka). Ophiolites are considerably less prone to chemical surface weathering compared to limestones suggesting that the impact of limestone surface weathering may be less critical over shorter timescales. Thus, cosmogenic ^{36}Cl exposure dating is likely to be able to distinguish between glacier formation events during Late Pleistocene intervals such as the LGM and the Late-glacial and could therefore be applied for the absolute dating of Unit 3 deposits.

However, limestone surfaces are highly susceptible to weathering, and determining surface erosion rates remains challenging. This limits the precision of the technique and renders it unsuitable for older deposits, such as those of Units 1 and 2. Particularly, Middle Pleistocene moraines are too old to be accurately dated using cosmogenic exposure dating, due to problems of rock surfaces erosion as well as boulder exhumation which are proved to yield much younger exposure ages than



Fig. 13. Google Earth view of the northern slopes of Mikros Trocharis, showing the locations of the discussed fans (A–C). The upper zone consists of white recrystallized limestones overlying black dolomites, while the lower zone is dominated by grey limestones. L and G indicate the entrances to Lion Cave and Gourgouthakas Cave, respectively.

the real ages of the moraines (Allard et al., 2020). So far, the dating of the Middle Pleistocene moraines has relied on U-series dating of secondary carbonate cements, which provide useful age bracketing of the moraines into different glacial cycles. However, whilst useful in recognising the presence of Middle Pleistocene glaciations in Greece and the wider Balkans, the U-series approach for dating secondary carbonates in moraines lacks precision on the actual age of the glaciations since the technique dates cements that form in succeeding interglacials of interstadials. This is because the precipitation of calcite is promoted by high temperatures and high evaporation rates since CO_2 is less soluble and more easily degassed at high temperatures. This, as well as high rates of evaporation, increase the concentration of calcium and bicarbonate ions in the water. In addition, a respiring surface soil increases carbon dioxide outgassing from carbonate-rich waters and promotes cement precipitation. These facts suggest that cement formation would have been favoured during interglacial or interstadial climates and helps to bracket moraines into different cold stages (Hughes, 2004). Given this reasoning, Late Pleistocene moraines will most likely contain secondary carbonates dating from the Holocene, limiting the usefulness of the U-series technique for precisely dating the last glaciation. Instead, ^{36}Cl exposure age dating is probably the best approach for dating Late Pleistocene moraines in the case of limestone terrains, whereas the technique is not viable for older Middle Pleistocene moraines due to surface weathering. So for older glacial deposits, U-series dating provides the best approach and ideally both U-series and ^{36}Cl exposure dating should be applied to assess the age of the glacial sequence (e.g. Hughes et al., 2006a; Allard et al., 2020; Pope et al., 2017, 2023). However, on Mt. Ida, there is no evidence indicating the presence of secondary precipitated calcites, making the application of the U-series technique for the absolute dating of Unit 1 & Unit 2 particularly challenging. Future research planned by the authors will apply ^{36}Cl exposure dating to test the age of the moraine, although as noted above the success of this approach depends on the age of the moraine with older surfaces particularly difficult to date.

5.2. The Quaternary glaciation of Crete within a regional paleoclimatic perspective

Glacial geomorphological evidence from Crete suggests that conditions for glacier formation during the Late Quaternary were extremely marginal. Although the occurrence of glaciers at such low latitudes and elevations in the Mediterranean underscores the role of increased precipitation as a key driver of glaciation, the evidence indicates that glaciers developed only in highly localized topoclimatic settings. On Mt. Ida, glacier formation was confined to a gently inclined slope within a tectonic-karstic amphitheater on the mountain's northern flank. This setting, characterized by substantial topographic shading and accumulation of wind-blown or avalanched snow, appears to have offset the otherwise unfavorable regional climatic conditions. The absence of glacial or periglacial features elsewhere on Mt. Ida further highlights the inadequacy of regional climatic conditions alone to support glaciation. Regional equilibrium-line altitudes (ELAs) must have lain close to the highest summits, in alignment with glacial reconstructions from mainland Greece. While latitude alone does not control ELAs—particularly in mainland Greece, where precipitation gradients dominate (Woodward and Hughes, 2011; Leontaritis et al., 2020)—the rise in ELAs from the Peloponnese to Crete could also be linked to the climatic buffering and moisture-modulating effects of the open sea.

A comparison of reconstructed ELAs can potentially reveal patterns in regional climatic evolution between the Middle Pleistocene and the LGM. During the Middle Pleistocene (MIS 12), the mean ELA difference between Mt. Chelmos (1967 m a.s.l.; 37.57°N) and Mt. Tymphi (1741 m a.s.l.; 39.59°N) was approximately 225 m, despite only a $\sim 2^\circ$ difference in latitude (see Introduction for references). Situated roughly 2.5° farther south ($\approx 35.15^\circ\text{N}$), the mountains of Crete would be expected to have ELAs exceeding 2200 m a.s.l. However, whereas ELAs of ice caps are largely independent of slope orientation and wind redistribution effects, cirque glaciers—such as those on Mt. Ida—are strongly influenced by wind-transported snow, which can result in locally depressed

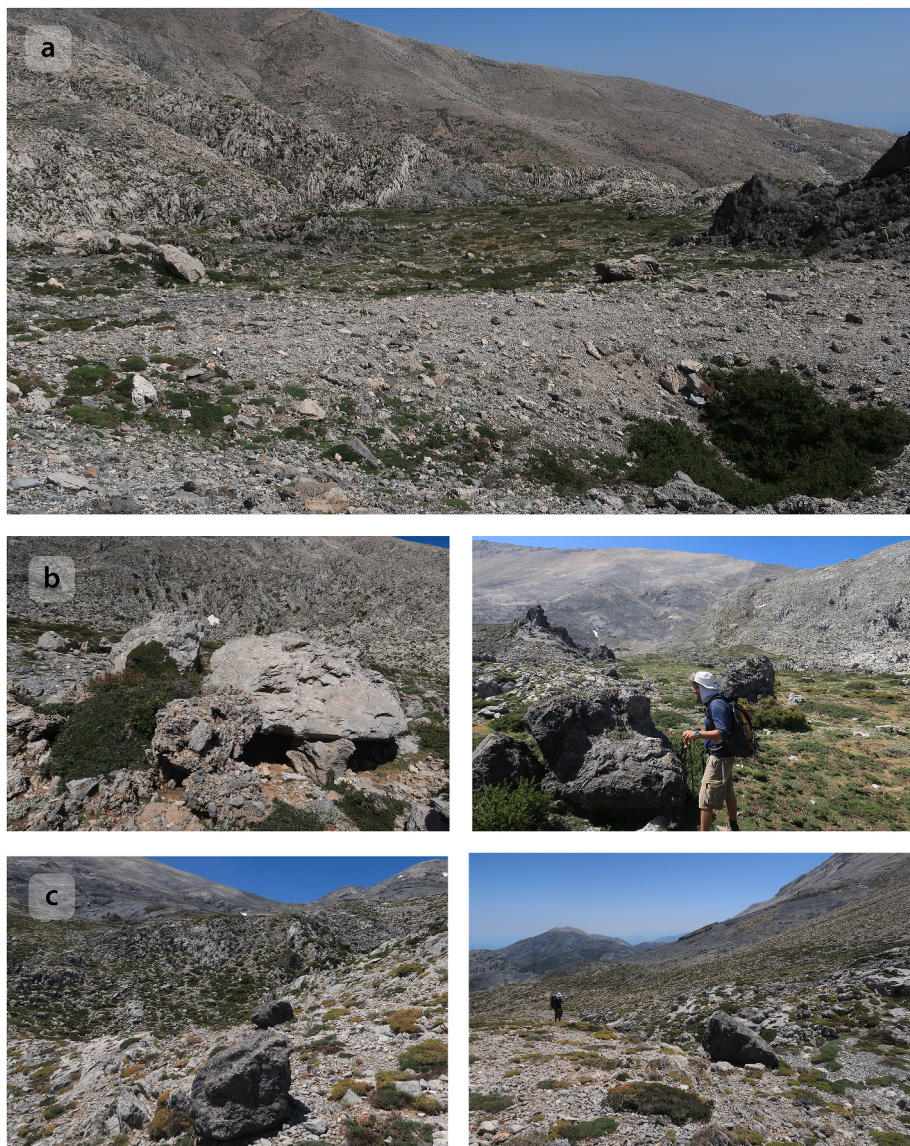


Fig. 14. a-b) Fan A is scattered with large boulders of various lithologies, suggesting deposition by high-energy processes, although no evidence supports a glacial or glacioluvial origin; c) Black dolomite boulders resting on grey limestones near the entrance of Gourgouthakas Cave. The transportation distance from the nearest black dolomite outcrop exceeds 300 m, indicating a high-energy transportation process. No evidence suggests they are glacially transported erratics.

ELAs (Bakke and Nesje, 2011). Thus, the calculated ELA of approximately 2073 m a.s.l., inferred from glacier reconstructions of the stratigraphically oldest and most extensive glacial phase on Mt. Ida, aligns with the broader pattern observed across mainland Greece.

By the LGM, this north–south gradient had markedly diminished. The ELAs on Mt. Chelmos (2046 m a.s.l.) and Mt. Tymphi (2016 m a.s.l.) differed by just 30 m (see Introduction for references), possibly indicating that increased aridity in northern Greece—and likely an accompanying south-westerly moisture flux toward southern Greece—compressed the latitudinal ELA gradient. This pattern is consistent with paleoatmospheric circulation models, which suggest a dominant southwest–northeast moisture flux delivering enhanced precipitation to the region (Kutzbach et al., 2014; Luetscher et al., 2015; Monegato et al., 2017; Wagner et al., 2019; Leontaritis et al., 2020).

Independent glacier reconstructions in the western Taurus Mountains in southwestern Turkey, approximately 450 km northeast of Mount Ida, support this interpretation. These reconstructions indicate conditions that were colder and significantly wetter than today (Sarıkaya et al., 2008), in contrast to the drier-than-present conditions reconstructed for the Kaçkar Mountains in northeastern Turkey (Keserci et al.,

2023; Sarıkaya et al., 2014). Evans et al. (2021) emphasize the importance of prevailing westerly and southwesterly winds from the Mediterranean in driving glaciation in Turkey during the LGM, contributing to the observed rise in ELAs and cirque floor elevations both eastward along the western Taurus range and northward inland from the coast.

The importance of westerly circulation on glacier ELAs across the Mediterranean is replicated in other glacier records across the region from Iberia to the Lebanon. This was observed in the comprehensive analysis of Mediterranean Pleistocene snowlines by Messerli (1967) and reinforced in a more recent review by Hughes and Woodward (2017). Similar analyses have also been presented at a regional level for Italy, Albania and Greece (Boenzi and Palmentola, 1997; Woodward and Hughes, 2011). Patterns of glaciation were affected through time by shifting positions of the North Atlantic Polar Front which was situated to the west of Iberia during the Last Glacial Cycle and through Termination I (Ruddiman and McIntyre, 1981a, 1981b). This is illustrated in the results of general circulation models, such as PMIP-2 which shows that at the LGM, the mid-latitude westerly belt was pushed southward in response to the ice sheet and sea ice extent at northern high latitudes (Laîné et al., 2009). The similarity between former glaciers ELAs and

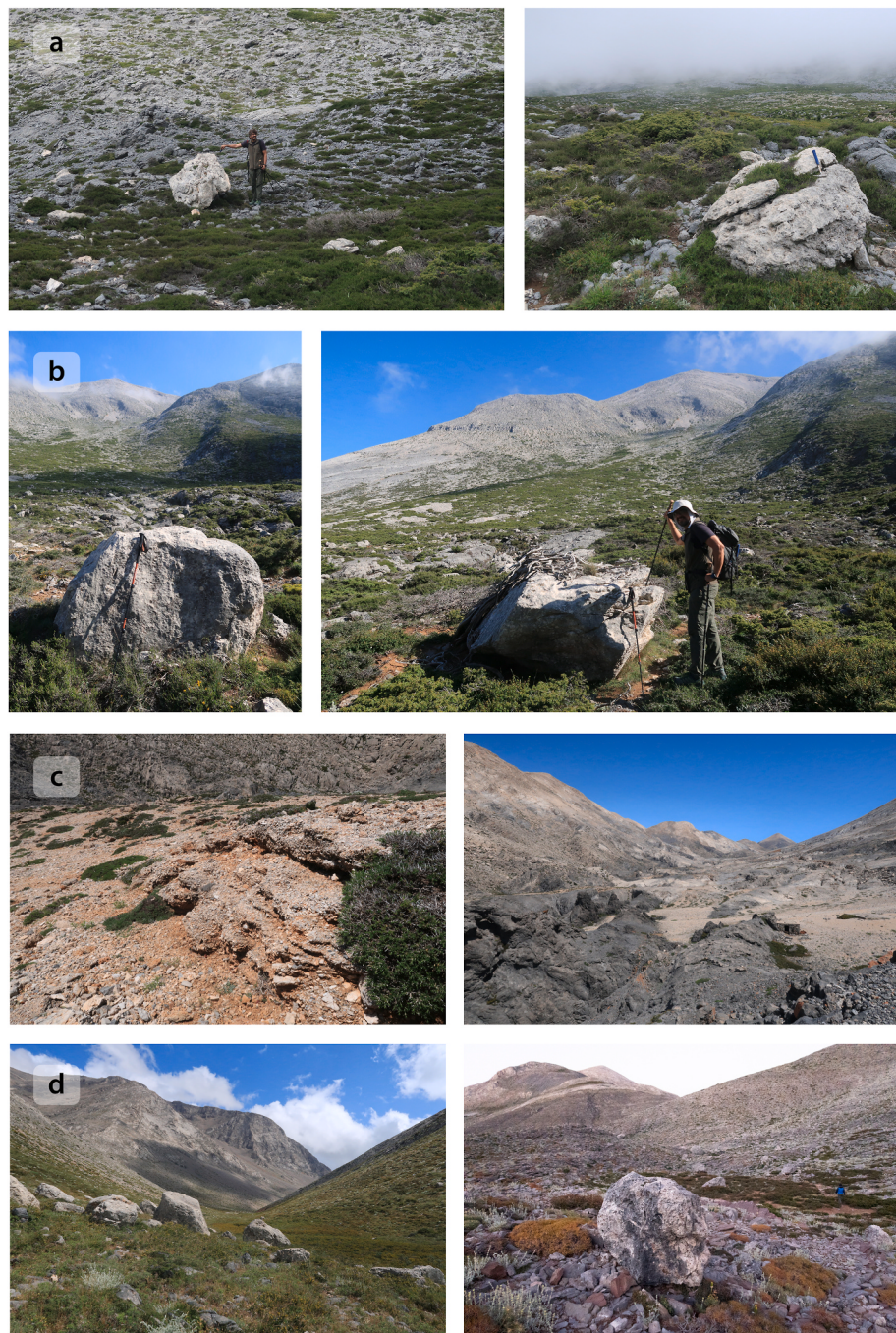


Fig. 15. **a)** Large white recrystallized limestone boulders originating from the higher sections of the overlying slopes near alluvial fan B; **b)** Similar boulders are closely deposited within alluvial fan C.; **c)** Typical alluvial fans in the Ammoudsera valley, located in the south-central highlands of Lefka Ori within the black dolomites and white marbles zone. These fans are typically composed of semi-sorted, finer, and more angular sediments, as illustrated in the left image, which shows a close-up of the alluvial fan seen in the right image; **d)** Rockfall boulders resting on alluvial fans and sediment traps within the thin-bedded limestone zone. The left image shows boulders in the large valley below the peak of Mavri Gourgoutha, while the right image shows impact marks on a recently fallen boulder in the Livada area.

modern precipitation isohyets reinforces the assertion that the drivers of moisture supply were the same in the Pleistocene as they are today, with westerly circulation controlling moisture supply through the Mediterranean (Florineth and Schlüchter, 2000) and consequently controlling ELA patterns (Hughes and Woodward, 2017; Rea et al., 2020; Hughes, 2022). However, whilst patterns of precipitation were similar to today, the amounts of precipitation varied. For example, when glaciers were at their largest during the Late Pleistocene the easternmost Mediterranean was drier than today (Moulin et al., 2022) whereas NW Greece received

similar precipitation to today (Hughes et al., 2006c).

The findings reported in this paper from Crete indicate that during the LGM, enhanced southwesterly moisture fluxes enabled glaciers in southern Greece to persist at ELAs comparable to, or only marginally higher than, those farther north. Should the most recent glacial phase on Mt. Ida is also confirmed to be LGM in age - as suggested by relative dating and the correlations presented here - the limited variation in ELAs across mainland Greece and Crete (approximately 2100 m a.s.l.) would further substantiate a southward trend toward increasingly wet climatic

conditions. Consequently, obtaining absolute dates for this glacial phase is essential for refining these regional comparisons and for elucidating the broader paleoclimatic significance of the Mount Ida glacial sequence.

5.3. The puzzling absence of pronounced glacial features in Lefka Ori

No evidence of glacial activity was identified in the Lefka Ori massif, in agreement with the conclusions of previous studies (Poser, 1957; Bonnefont, 1972; Boenzi and Palmentola, 1982; Fabre and Maire, 1983; Maire, 1990b; Rackham and Moody, 1996). The prominent open U-shaped valleys in the region were determined not to be of glacial origin. Instead, their morphology suggests a polygenetic development, predominantly shaped by karstification. This process was likely enhanced by active Pleistocene tectonism, which further compartmentalized inherited karst surfaces and depressions. Extensive karst features in the Lefka Ori massif are closely associated with exposures of the older Lower Plattenkalk Unit. These unique lithological characteristics, combined with substantial orographic precipitation, appear to have played a significant role in driving this geomorphological evolution.

A few alluvial fans containing large boulders are located at the base of steep, high-elevation, north-facing slopes in the northeastern part of the massif. These fans exhibit characteristics consistent with high-energy fluvial processes, while the presence of large boulders within them is attributed to a combination of rockfalls and fluvial transport. However, there is no direct evidence linking these fans and boulders to glacial activity, nor is there other evidence to suggest that this part of Lefka Ori was glaciated. This observation is also true for the well-documented Sfakia fan in the southern piedmont of the massif. While earlier studies have proposed a relationship between glaciation and fan formation (e.g., Nemeć and Postma, 1993), recent research has demonstrated that the formation of the Sfakia fans was not significantly influenced by glaciation (Ott et al., 2023, p. 388).

The following discussion analyzes possible climatic, geomorphological and geological explanations for the absence of glaciers during the Pleistocene cold stages in the massif of Lefka Ori.

5.3.1. ELAs and paleoprecipitation in the mountains of Crete

The massifs of Ida and Lefka Ori share similar altitudes and latitudes, placing them in the same air-temperature zone. Therefore, any differences in their theoretical ELAs during the glacial stages of the Quaternary could be attributable to variations in precipitation (see Ohmura and Boettcher, 2018, and references therein). The presence of a small glacier on Mt. Ida, contrasted with the absence of glaciers on Lefka Ori, likely suggests that theoretical ELAs over Lefka Ori could have been higher than those on Mt. Ida. This could be attributed, at least in part, to differences in precipitation between the two massifs, with Mt. Ida likely receiving relatively higher precipitation.

Such a discrepancy may point to variations in past precipitation patterns, potentially driven by an atmospheric circulation regime distinct from that of the present day. Mt. Ida, located 70 km further east than Lefka Ori, currently experiences drier conditions due to prevailing westerly precipitation-bearing winds. Its position relative to the coast is not significantly different from Lefka Ori, though it is slightly further inland (20–30 km for Mt. Ida compared with 5–10 km for Lefka Ori), which is a minor difference at the regional scale. In contrast, prevailing winds from the south or southwest, associated with depressions moving through the Mediterranean, would have brought significant precipitation as air from the Libyan Sea encountered the orographic barriers of Ida and Lefka Ori, making both massifs at least equally wet. These observations should, in any case, be viewed with caution and considered alongside other parameters that may have affected glaciation in Crete, as discussed below.

5.3.2. Geomorphology

While the estimated ELAs do not rule out past glaciation in the Lefka

Ori, any glaciers would likely have been small and localized, due to the limited area above these altitudes and the modest elevation of the highest peak (2453 m a.s.l.). Notably, in contrast to Mt. Ida, which features a well-defined west–east ridgeline, the highlands of Lefka Ori comprise a diffuse plateau at 1700–2000 m a.s.l., with numerous conical peaks rising above 2200 m a.s.l. (Fig. 16a–b). This plateau generally lacks extensive north-facing slopes with topographic configurations favorable for the accumulation of windblown or avalanching snow. As a result, the region offers few locations with local topoclimatic advantages necessary for sustained ice accumulation and glacier development.

To evaluate this further, the high-elevation areas (>1600 m a.s.l.) of Lefka Ori and Mt. Ida were analyzed, focusing on slope orientation and extent. Slopes with orientations within 30° of due north—similar to the glaciated Migeros slope on Mt. Ida—were classified to identify potentially favorable topographies for glaciation and to facilitate comparison with the Migeros slope (Fig. 16e–f). On Mt. Ida the Migeros area and its adjacent slopes (labeled M and AM in Fig. 16f) were the only significant cluster of long, north-facing slopes within the massif. In Lefka Ori, five representative slope clusters (labeled W, S, C, T, and E in Fig. 16e) were selected based on their orientation and extent, spanning the two primary lithological units. Notably, Lefka Ori and Mt. Ida differ significantly in lithology (Fig. 16c–d).

Importantly, even within Mt. Ida, not all north-facing slopes show evidence of glaciation. The slopes adjacent to the Migeros cirque, despite sharing similar orientation and position below the ridgeline, appear to have remained unglaciated. To investigate the geomorphological differences, longitudinal topographic profiles were compared for three representative slopes on each site (Fig. 16g–h). The key distinction lies in the gentler inclination of the glaciated Migeros slope (M profile), in contrast to the steeper, non-glaciated slopes (AM profile). Similarly, in Lefka Ori, the most extensive north-facing slopes are steep, while gentler, non-glaciated valleys—such as E and W in Fig. 16g–h—are notably less extensive.

Moreover, it is striking that Migeros is the only extensive, north-facing valley across both massifs that is gently inclined and contains (karstic) hollows conducive to ice accumulation. The Migeros cirque and valley is situated within a tectonic valley formed by the intersection of two normal faults. The steep northern slope of Mt. Ida ridge is primarily shaped by an E–W trending normal fault, likely of Late Miocene age (Fassoulas, 1999), which also defines the Migeros plateau as a small tectonic graben. Superimposed on this structure are younger, NW–SE trending normal faults, which exhibit a notable residual lateral component and intersect the older fault system, creating a tectonic amphitheater where the cirque has developed (Fig. 4; Fassoulas, 2001).

This analysis highlights that, in addition to climatic factors such as precipitated, avalanching, and wind-transported snow, and topographic shading, geomorphological features—such as topographic shading, gentle slopes, and inherited glaciokarst depressions—likely played a critical role in enabling glacier formation under marginal conditions. Furthermore, the presence of a cirque and an ice-scoured valley provides a more favorable landscape for glacier formation during subsequent glacial periods. This geomorphological advantage may explain why a small glacier formed on Mt. Ida, but not in Lefka Ori, as also suggested by Maire (1990b).

5.3.3. Tectonic uplift history

A crucial yet often overlooked factor in discussions of relict glacial topography across different geographical settings is the role of tectonic uplift in shaping paleoelevations during past glaciations, particularly in tectonically active regions such as Crete. Glacial modeling in tectonically active regions has not adequately accounted for uplift dynamics, which can significantly impact glacial reconstructions (Giraudi and Giacco, 2015; Leontaritis, 2021; Leontaritis et al., 2022). Crete lies within the uplifted forearc of the Hellenic subduction margin, where the African Plate subducts beneath the Aegean microplate, creating a highly active tectonic environment. Consequently, although the Ida and Lefka

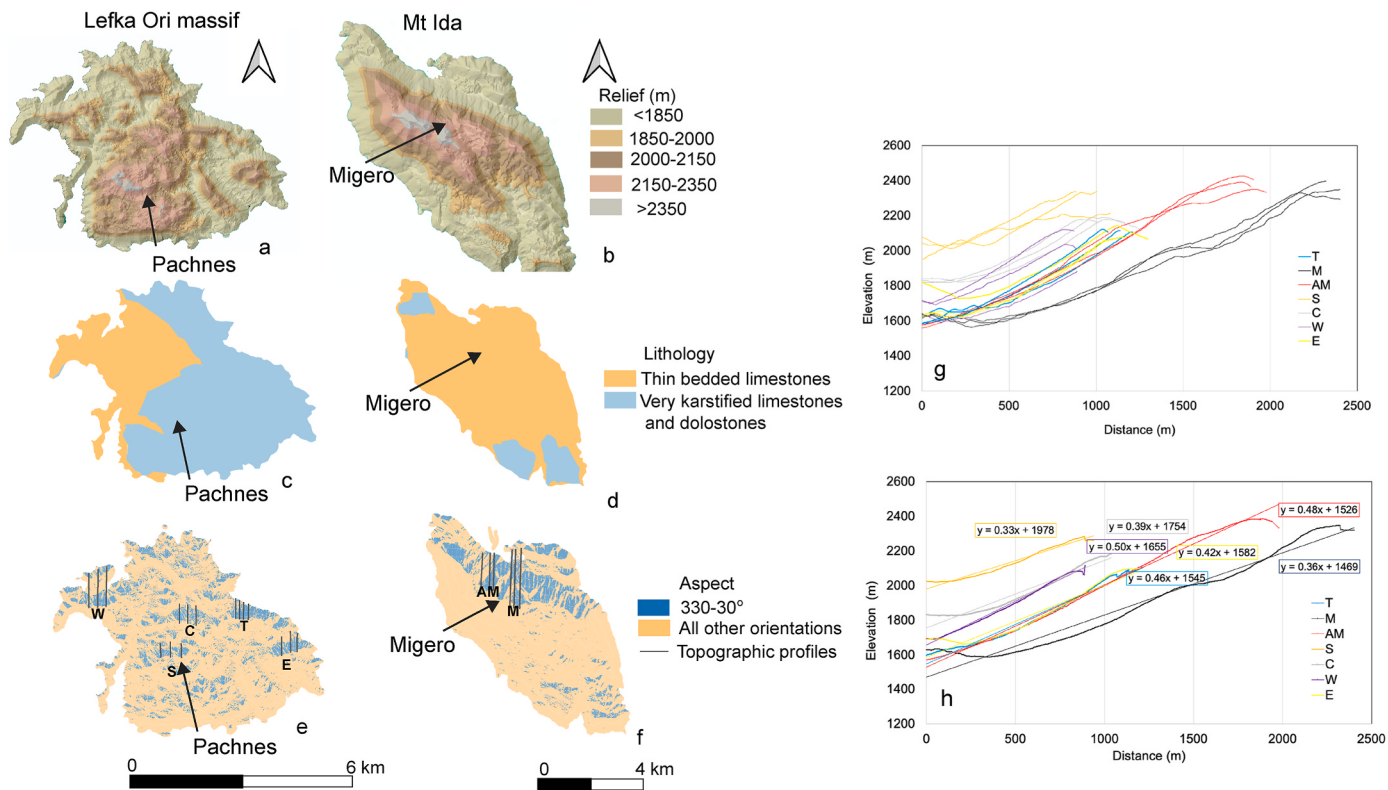


Fig. 16. Topographical analysis of the Lefka Ori (a, c, e) and Mt. Ida (b, d, f) highlands (>1600 m a.s.l.). The locations of the analyzed areas are shown in Fig. 3. a-b) Relief analysis; c-d) Lithological classification distinguishing Eocene thin-bedded limestones from Triassic limestones and dolostones, based on Creutzburg et al. (1977) and Vidakis et al. (1993), with modifications according to the suggestions of Papanikolaou and Vassilakis (2010) and Moraetis et al. (2025); e-f) Slope aspect classification; g) Longitudinal topographic profiles of slopes shown in panels (e) and (f); h) Average longitudinal topographic profiles for each region with corresponding linear regression fitting. The slope coefficient a approximates the inclination angle as $\tan^{-1}(a)$.

Ori massifs are currently at similar elevations, their heights may have differed in the past due to variations in tectonic uplift rates over time. In addition to the direct influence of paleoelevations on glacier formation, paleoprecipitation in the two massifs would also have been significantly affected, with consequent impacts on the equilibrium line altitudes (ELAs). This inference is supported by modern observations from Crete, where precipitation exhibits an exponential increase with elevation (Tzoraki et al., 2015; Climatic Atlas of Greece, 2020). Given the relatively high ELAs and the marginal conditions for glaciation on Crete, even modest variations in paleoelevations could have played a critical role in glacier formation.

Roberts et al. (2013) analyzed approximately 250 longitudinal river profiles to reconstruct the spatial and temporal history of Crete's uplift rates over the past 5 million years (Ma). Their findings indicate that Crete began uplifting between ~4 and 2 Ma at rates of ~0.1–0.5 mm/yr. Uplifting in central Crete initiated around ~4 Ma (Meulenkamp et al., 1994), with eastern and western Crete following 1–2 million years later (Roberts et al., 2013). Despite temporal differences, cumulative uplift over the last 1 Ma has been similar in regions encompassing the Lefka Ori and Ida massifs (Roberts et al., 2013). The highest average uplift rates occurred between 0 and 1 Ma, with central and western Crete reaching rates of up to 1–1.2 mm/yr (Roberts et al., 2013).

These observations align with optically stimulated luminescence (OSL) dating of paleoshorelines (142–68 ka), which indicate average uplift rates of 0.5–1.1 mm/yr along the southern shoreline of central and western Crete during the Late Pleistocene and Holocene (Angelier, 1979; Ott et al., 2019). More recent constraints, based on ^{36}Cl exposure dating of wave-cut platforms coupled with uplift modeling, suggest paleoshoreline uplift rates in southwestern Crete have remained constant at ~0.61–0.83 mm/yr since ~400 ka (Robertson et al., 2023). However, the applicability of ^{36}Cl exposure dating for terraces older than 50 ka has

been questioned (see prior discussion on ^{36}Cl dating of glacial deposits), and these estimates should be interpreted cautiously. Furthermore, several other studies highlight significant temporal variations in uplift rates (Gallen et al., 2014; Mouslopoulou et al., 2015a,b; Tiberti et al., 2014).

Despite uncertainties in determining uplift rate variability using different dating methods, the presence of submerged archaeological sites in eastern Crete, contrasted with elevated sites of the same age in western Crete, provides clear evidence of differential uplift between the two regions at specific periods (Antonioli et al., 2007; Mouslopoulou et al., 2015a,b and references therein). Further supporting this contrast, the 365 AD paleoshoreline exhibits an elevation difference of 10 m over a 100 km distance from west to east (Mouslopoulou et al., 2015a). Additionally, evidence from the well-preserved alluvial fan system at the mouth of the Klados Gorge (western Crete) suggests that uplift rates exceeded sea-level rise rates, preventing the fan sequence from being eroded by wave action (Mouslopoulou et al., 2015a, 2017; Tiberti et al., 2014). While the age of these fans remains debated, with estimates ranging from the Late Pleistocene to the Middle-Late Holocene (Bruni et al., 2021; Mouslopoulou et al., 2017), their preservation strongly indicates high uplift rates in western Crete. These findings are consistent with previous studies indicating fluctuating uplift rates over the past 20 ka, locally reaching as high as 2–8 mm/yr (Mouslopoulou et al., 2016, 2017; Pirazzoli et al., 1982, 1996; Shaw et al., 2008; Tiberti et al., 2014).

Overall, southwestern Crete, including the Lefka Ori massif, has undergone intense uplift since the LGM, with particularly high rates during the Holocene (e.g., Lambeck, 1995; Price et al., 2002, and references therein). In contrast, Mt. Ida, located further inland, displays more subdued tectonic activity compared to the southern coastal zone (Price et al., 2002; Ganias and Parsons, 2009, and references therein). Late Pleistocene to Holocene uplift rate estimates for Mt. Ida is limited

but are generally inferred to be slower than those in western Crete's coastal regions (Ganas and Parsons, 2009; Caputo et al., 2010, and references therein). The pronounced recent uplift disparity between the Lefka Ori and Mt. Ida is further evidenced by the numerous deep gorges dissecting the southern flanks of the Lefka Ori, in contrast to the comparatively fewer and less pronounced gorges observed on Mt. Ida and across central Crete (Fassoulas et al., 2004; Fassoulas and Nikolaikakis, 2005).

Given that average uplift rates over the past 1 Ma are comparable between Mt Ida and Lefka Ori (Roberts et al., 2013; Ott et al., 2019), it is plausible that Lefka Ori experienced a larger share of its cumulative uplift during the Late Quaternary, supported by ongoing tectonic activity and high Late Pleistocene to Holocene uplift rates in southwestern Crete. Conversely, Mt Ida may have undergone a greater proportion of its uplift prior to the Middle Pleistocene glaciation, although additional data are required to constrain the local uplift rates, particularly given its more inland position. This likely resulted in differing paleo-elevations of the two massifs during glacial periods. Given the marginal conditions for glaciation and the high ELAs, these elevation differences could also provide an explanation for the absence of glaciers on Lefka Ori during the Middle to Late Pleistocene glacial phases.

The extent to which differences in tectonic uplift rates between eastern and western Crete influence variations in theoretical ELAs remains uncertain. However, persistent spatial and temporal variations in uplift rates could lead to elevation differences of several hundred meters over extended timescales (see discussion in Leontaritis, 2021). For instance, assuming an uplift rate difference of ~2–4 mm/yr over the past 25 ka between the examined massifs, Mt Ida would have been approximately 50–100 m higher than Lefka Ori during the LGM. This elevation difference could have been even more significant during the more severe Middle Pleistocene glacial phases (e.g. MIS6; MIS 12), even when accounting for smaller disparities in average uplift rates. Indicatively, an uplift rate difference of ~0.2–0.4 mm/yr over the past 500ka would have resulted in an additional 100–200m relative elevation difference between the two massifs during the MIS 12 glaciation. These estimates are indicative and cannot be directly inferred from the available data. However, they underscore the potential influence of tectonic activity on glacial evolution and the importance of accounting for tectonic uplift disparities in reconstructing past glaciations in these massifs.

6. Conclusions

This study presents the first detailed field investigation of Quaternary glaciations in the mountains of Crete, focusing on the Ida (2456 m a.s.l.) and Lefka Ori (2453 m a.s.l.) massifs, located in central and western Crete, respectively.

Our results provide robust evidence for three distinct glacial phases in Mt. Ida, characterized by a well-preserved glacial sequence within a characteristic cirque-moraine system. In contrast, Lefka Ori lacks definitive glacial features, and the topoclimatic conditions have most probably been unfavorable for sustained glacier formation. Consequently, our findings rule out significant Quaternary glaciation in Lefka Ori, highlighting a spatial limitation in the extent of glaciation across Crete.

A relative chronology for the glacial phases on Mt Ida is proposed within the well-established chronostratigraphic framework of glaciations recognized in the mountains of Greece, suggesting correlation with glaciations during the Middle Pleistocene (MIS 12 and MIS 6) and the LGM. On Mt. Ida, local topoclimatic conditions were critical for glacier development under marginal climatic conditions, with reconstructed regional ELAs ranging from approximately 2070 to 2100 m a.s.l. — a pattern consistent with glacial reconstructions across mainland Greece. At a broader paleoclimatic scale, absolute dating of the youngest glacial phase on Mt. Ida is necessary to confirm whether it corresponds to the LGM. If so, this would support the hypothesis of wetter climatic conditions in southern Greece and western Turkey during the LGM,

potentially driven by paleoatmospheric circulation patterns that supplied moisture along a more southwest–northeast trajectory than at present.

No additional significant glacial features were identified on either Mt. Ida or Lefka Ori, aligning with findings from previous studies. An analysis of the profiles of prominent open U-shaped valleys in the Lefka Ori indicates that they are not of glacial origin; rather, their blind sections suggest a predominantly karstic, endorheic drainage system. This morphology supports a polygenetic landscape evolution, with karstification playing a dominant role. The absence of prominent glacial features in the Lefka Ori massif, despite its greater size and higher modern precipitation compared to Mt. Ida, is particularly notable. This discrepancy likely reflects a combination of factors. Even if prevailing winds from the south or southwest would have made both massifs at equally wet, preliminary geomorphological analysis suggests that the Lefka Ori highlands lack the topographic configurations necessary for sustained ice accumulation and glacier formation. Tectonic factors also appear to have played a key role. Uplift histories suggest that Lefka Ori underwent more rapid uplift during the Late Quaternary, while Mt. Ida experienced greater uplift prior to the Middle Pleistocene glaciations. These differences likely affected paleoelevations during glacial periods. Given the marginal conditions for glaciation and elevated ELAs across Crete, even modest elevation disparities may have critically influenced glacier extent and persistence. These findings highlight the importance of accounting for long-term tectonic evolution when reconstructing glacial histories in Crete and other tectonically active regions of the Mediterranean.

Declaration of competing interest

The authors declare that they have no known competing financial interests or personal relationships that could have appeared to influence the work reported in this paper.

Acknowledgements

The project was partially funded by IUGS and UNESCO through the IGCP-715 initiative. We would like to thank Dr. Maria Kolendrianou, Dr Fabian Kirste and Emmanouel Nikolakakis for their help with field data collection on Mt. Ida. We also appreciate the support and hospitality of Assoc. Prof. George Chasapis, Aspasia Anagnostopoulou, Fotini Kokkali, George Makrydakis, and Alonia Guesthouse during our field surveys in the mountains of Crete. Our sincere thanks go to Dr. Roza Avgouli for her contributions to graphic design and to Anavasi Editions for providing cartographic material. Finally, we thank Ian Evans (Durham University) for his valuable comments on an earlier draft of this paper.

Data availability

All data and/or code is contained within the submission.

References

- Adamopoulos, K., 2005. The deepest and the longest caves in Greece. In: Proceedings of the 14th International Congress of Speleology, 21–28 August. Kalamos, Athens, Greece.
- Adamopoulos, K., 2013. 1000 and 1 caves in "Lefka Ori" massif on Crete, Greece. In: Filippi, M., Bosák, P. (Eds.), Proceedings of the 16th International Congress of Speleology, pp. 273–278. Brno, Czech Republic.
- Akçar, N., Yavuz, V., Yeşilyurt, S., Ivy-Ochs, S., Reber, R., Bayrakdar, C., Kubik, P.W., Zahno, C., Schlunegger, F., Schlüchter, C., 2017. Synchronous last glacial maximum across the Anatolian peninsula. Geological Society, London, Special Publications 433 (1), 251–269. <https://doi.org/10.1144/SP433.14>.
- Alfimov, V., Ivy-Ochs, S., 2009. How well do we understand production of 36Cl in limestone and dolomite? *Quat. Geochronol.* 4 (6), 462–474. <https://doi.org/10.1016/j.quageo.2009.08.005>.
- Allard, J.L., Hughes, P.D., Woodward, J.C., Fink, D., Simon, K., Wilcken, K.M., 2020. Late Pleistocene glaciers in Greece: a new 36Cl chronology. *Quat. Sci. Rev.* 245, 106528. <https://doi.org/10.1016/j.quascirev.2020.106528>.

- Anavasi, 2023. Ida (Mt Ida), Hiking Map 1:30,000. Anavasi Maps & Guides [Topo 25, Crete 11.14].
- Anavasi, 2024. Leuka Ori (White Mountains), Hiking Map 1:25,000. Anavasi Maps & Guides [Topo 25, Crete 11.11/11.12].
- Angelier, J., 1979. Néotectonique de l'Arc égéen. *Soc. Geol. Du Nord* 3, 418.
- Antonioli, F., Anzidei, M., Lambbeck, K., Auriemma, R., Gaddi, D., Furlani, S., Orrù, P., Solinas, E., Gaspari, A., Karinja, S., Kovacic, V., Surace, L., 2007. Sea-level change during the Holocene in Sardinia and in the northeastern Adriatic (central Mediterranean Sea) from archaeological and geomorphological data. *Quat. Sci. Rev.* 26 (19–21), 2463–2486. <https://doi.org/10.1016/j.quascirev.2007.06.022>.
- Augustinus, P.C., 1992. The influence of rock mass strength on glacial valley cross-profile morphometry: a case study from the Southern Alps, New Zealand. *Earth Surf. Process. Landf.* 17 (1), 39–51. <https://doi.org/10.1002/esp.3290170104>.
- Augustinus, P.C., 1995. Glacial valley cross-profile development: the influence of in situ rock stress and rock mass strength, with examples from the Southern Alps, New Zealand. *Geomorphology* 14 (2), 87–97. [https://doi.org/10.1016/0169-555X\(95\)00050-X](https://doi.org/10.1016/0169-555X(95)00050-X).
- Bakke, J., Nesje, A., 2011. Equilibrium-Line Altitude (ELA). In: Singh, V.P., Singh, P., Haritashya, U.K. (Eds.), *Encyclopedia of Snow, Ice and Glaciers. Encyclopedia of Earth Sciences Series*. Springer, Dordrecht. https://doi.org/10.1007/978-90-481-2642-2_140.
- Bathrellos, G.D., Skilodimou, H.D., Maroukian, H., 2014. The spatial distribution of Middle and Late Pleistocene cirques in Greece. *Geogr. Ann. Phys. Geogr.* 96 (3), 323–338.
- Bathrellos, G.D., Skilodimou, H.D., Maroukian, H., 2015. The significance of tectonism in the glaciations of Greece. In: Siart, C., Bini, B., Bras, R. (Eds.), *Geological Society, London, Special Publications* 433 (1), 237–250. <https://doi.org/10.1144/sp433.5>.
- Benn, D.I., Hulton, N.R.J., 2010. An Excel™ spreadsheet program for reconstructing the surface profile of former mountain glaciers and ice caps. *Comput. Geosci.* 36 (5), 605–610. <https://doi.org/10.1016/j.cageo.2009.09.016>.
- Bergmeier, E., 2002. The vegetation of the high mountains of Crete: a revision and multivariate analysis. *Phytocoenologia* 32 (2), 205–249. <https://doi.org/10.1127/0340-269X/2002/0032-0205>.
- Bernard, M., Steer, P., Gallagher, K., Egholm, D.L., 2021. The impact of lithology on fjord morphology. *Geophys. Res. Lett.* 48, e2021GL093101. <https://doi.org/10.1029/2021GL093101>.
- Blair, T.C., McPherson, J.G., 1995. Quaternary alluvial fans in southwestern Crete: Sedimentation processes and geomorphic evolution. *Sedimentology* 42 (3), 531–535. <https://doi.org/10.1111/j.1365-3091.1995.tb00390.x>.
- Boenzi, F., Palmentola, G., 1982. Aspetti geomorfologici del massiccio dei Leuka Ori nell'isola di Creta (Grecia), con particolare riguardo alle forme carsiche. *Geol. Appl. Idrogeol.* 17, 75–83.
- Boenzi, F., Palmentola, G., 1997. Glacial features and snow-line trend during the last glacial age in the southern Apennines (Italy) and on Albanian and Greek mountains. *Z. Geomorphol.* 41 (1), 21–29.
- Bonneau, M., 1984. Correlation of the Hellenic nappes in the southern Aegean and their tectonic reconstruction. In: Dixon, J.E., Robertson, A.H.F. (Eds.), *The Geological Evolution of the Eastern Mediterranean*. Geological Society, London, pp. 517–527. <https://doi.org/10.1144/GSL.SP.1984.017.01.38>.
- Bonneau, M., Jonkers, H.A., Meuleunkamp, J.E., 1984. *Geological Map of Greece 1:50,000, Timpakion Sheet*. Institute of Geological and Mineral Exploration.
- Bonnefont, J.C., 1972. *La Crète: Etude morphologique* (Doctoral Dissertation). Université de Lille III, France.
- Bruni, E.T., Ott, R.F., Picotti, V., Haghipour, N., Wegmann, K.W., Gallen, S.F., 2021. Stochastic alluvial fan and terrace formation triggered by a high-magnitude Holocene landslide in the Klados Gorge, Crete. *Earth Surf. Dyn.* 9, 771–793. <https://doi.org/10.5194/esurf-9-771-2021>.
- Caputo, R., Catalano, S., Monaco, C., Romagnoli, G., Tortorici, G., Tortorici, L., 2010. Active faulting on the island of crete (Greece). *Geophys. J. Int.* 183 (1), 111–126. <https://doi.org/10.1111/j.1365-246X.2010.04749.x>.
- Chandler, B.M.P., Lovell, H., Boston, C.M., Lukas, S., Barr, I.D., Benediktsson, I.Ö., Benn, D.I., Clark, C.D., Darvill, C.M., Evans, D.J.A., Ewertowski, M.W., Loibl, D., Margold, M., Otto, J.-C., Roberts, D.H., Stokes, C.R., Storrar, R.D., Stroeven, A.P., 2018. Glacial geomorphological mapping: a review of approaches and frameworks for best practice. *Earth Sci. Rev.* 185, 806–846. <https://doi.org/10.1016/j.earscirev.2018.07.015>.
- Climatic Atlas of Greece, 2020. Hellenic national meteorological service. <http://climatlas.hnms.gr/>.
- Creutzburg, N., Drooger, C.W., Meulenkamp, J.E., 1977. *General Geologic Map of Crete 1:200,000*. Institute of Geological and Mining Research (IGME).
- Evans, I.S., 2007. Glacial landforms, erosional features | major scale forms. In: Elias, S.A. (Ed.), *Encyclopedia of Quaternary Science*. Elsevier, pp. 838–852. <https://doi.org/10.1016/B0-44-452747-8/00098-3>.
- Evans, I.S., Çilgin, Z., Bayrakdar, C., Canpolat, E., 2021. The form, distribution and paleoclimatic implications of cirques in southwest Turkey (Western Taurus). *Geomorphology* 391, 107885. <https://doi.org/10.1016/j.geomorph.2021.107885>.
- Fabre, G., Maire, R., 1983. Néotectonique et morphogénèse insulaire en Grèce: Le massif du Mont Ida (Crète). In: Méditerranée, troisième série, tome 48 –2. Evolution récente des paysages de la péninsule hellénique, pp. 39–49. <http://geoprodig.cnrs.fr/it/ems/show/163280>.
- Fassoulas, C., 1999. The structural evolution of central Crete: Insight into the tectonic evolution of the South Aegean (Greece). *J. Geodyn.* 27 (1), 23–43.
- Fassoulas, C., 2001. The tectonic development of a Neogene basin at the leading edge of the active European margin: the Heraklion basin, Crete, Greece. *J. Geodyn.* 31 (1), 63–84. [https://doi.org/10.1016/S0264-3707\(00\)00017-X](https://doi.org/10.1016/S0264-3707(00)00017-X).
- Fassoulas, C., Nikolakakis, E., 2005. Landscape response to the tectonic uplift of Crete, Greece. *Bull. Geol. Soc. Greece* 37, 201–217.
- Fassoulas, C., Kiliias, A., Mountrakis, D., 1994. Postnappe stacking extension and exhumation of high-pressure/low-temperature rocks in the island of Crete, Greece. *Tectonics* 13 (1), 127–138. <https://doi.org/10.1029/93TC01955>.
- Fassoulas, C., Nikolakakis, E., Paragamian, K., 2004. Geomorphologic and tectonic features of Cretan gorges, Crete, Greece. *Proceedings of the 5th International Symposium on Eastern Mediterranean Geology* 1, 415–418.
- Ferrier, G., Pope, R.J.J., 2012. Quantitative mapping of alluvial fan evolution using ground-based reflectance spectroscopy. *Geomorphology* 175–176, 14–24. <https://doi.org/10.1016/j.geomorph.2012.06.013>.
- Florineth, D., Schlüchter, C., 2000. Alpine evidence for atmospheric circulation patterns in Europe during the last glacial maximum. *Quaternary Research* 54 (3), 295–308.
- Gallen, S.F., Wegmann, K.W., Bohnenstiel, D.R., Pazzaglia, F.J., Brandon, M.T., Fassoulas, C., 2014. Active simultaneous uplift and margin-normal extension in a forearc high, Crete, Greece. *Earth Planet Sci. Lett.* 398, 11–24. <https://doi.org/10.1016/j.epsl.2014.03.031>.
- Ganas, A., Parsons, T., 2009. Three-dimensional model of Hellenic Arc deformation and origin of the Cretan uplift. *J. Geophys. Res.* 114 (B06404). <https://doi.org/10.1029/2008JB005599>.
- Gouvas, M., Sakellariou, N., 2011. Climate and forest vegetation of Greece. In: National Observatory of Athens, Institute of Environmental Research and Sustainable Development, Technical Library Report Nr. 01/2011 (in Greek).
- Giraudi, C., Giaccio, B., 2015. Middle Pleistocene glaciations in the Apennines, Italy: new chronological data and preservation of the glacial record. In: Hughes, P.D., Woodward, J.C. (Eds.), *Quaternary Glaciation in the Mediterranean Mountains*, 433. Geological Society of London Special Publications, pp. 161–178. <https://doi.org/10.1144/SP433.1>.
- Hedding, D.W., Sumner, P.D., 2013. Diagnostic criteria for pronal ramparts: Site, morphological and sedimentological characteristics. *Geografiska Annaler: Series B, Human Geography* 95 (4), 315–322. <http://www.jstor.org/stable/43870695>.
- Hempel, L., 1991. *Forschungen zur Physischen Geographie der Insel Kreta im Quartär. Ein Beitrag zur Geokologie des Mittelmeerraumes*. Vandenhoeck Ruprecht, pp. 58–86.
- Hughes, P.D., 2004. Quaternary Glaciation in the Pindus Mountains, Northwest Greece. University of Cambridge. <https://doi.org/10.17863/CAM.20476>. PhD thesis.
- Hughes, P.D., 2010. Geomorphology and Quaternary stratigraphy: the roles of morpho-, litho-, and allostratigraphy. *Geomorphology* 123, 189–199. <https://doi.org/10.1016/j.geomorph.2010.07.025>.
- Hughes, P.D., 2022. The glacial landscapes of the Iberian Peninsula within the Mediterranean region. In: Gómez-Ortiz, J.J., Ballesteros Cánovas, J.A., Palacios, D. (Eds.), *Iberia, Land of Glaciers*. Elsevier, pp. 37–54. <https://doi.org/10.1016/B978-0-12-821941-6.00003-7>.
- Hughes, P.D., Gibbard, P.L., 2015. A stratigraphical basis for the last glacial maximum (LGM). *Quat. Int.* 383, 174–185. <https://doi.org/10.1016/j.quaint.2014.06.006>.
- Hughes, P.D., Woodward, J.C., 2009. Glacial and periglacial environments. In: Woodward, J.C. (Ed.), *The Physical Geography of the Mediterranean*. Oxford University Press, pp. 353–383.
- Hughes, P.D., Woodward, J.C., 2017. Quaternary glaciation in the Mediterranean mountains: a new synthesis. Geological Society, London, Special Publications 433, 1–23. <https://doi.org/10.1144/SP433.14>.
- Hughes, P.D., Gibbard, P.L., Woodward, J.C., 2003. Relict rock glaciers as indicators of mediterranean paleoclimate during the last glacial maximum (late würmian) of northwest Greece. *J. Quat. Sci.* 18, 431–440. <https://doi.org/10.1002/jqs.764>.
- Hughes, P.D., Woodward, J.C., Gibbard, P.L., Macklin, M.G., Gilmour, M.A., Smith, G.R., 2006a. The glacial history of the Pindus Mountains, Greece. *J. Geol.* 114, 413–434. <https://doi.org/10.1086/504177>.
- Hughes, P.D., Woodward, J.C., Gibbard, P.L., 2006b. The last glaciers of Greece. *Z. Geomorphol.* 50, 37–46. <https://doi.org/10.1127/zfg/50/2006/37>.
- Hughes, P.D., Woodward, J., Gibbard, P.L., 2006c. Late pleistocene glaciers and climate in the mediterranean. *Global Planet. Change* 50 (1–2), 83–98. <https://doi.org/10.1016/j.gloplacha.2005.07.005>.
- Hughes, P.D., Woodward, J.C., van Calsteren, P.C., Thomas, L.E., 2011. The glacial history of the Dinaric Alps, Montenegro. *Quat. Sci. Rev.* 30 (23–24), 3393–3412. <https://doi.org/10.1016/j.quascirev.2011.08.016>.
- Hughes, P.D., Woodward, J.C., van Calsteren, P.C., Thomas, L.E., Adamson, K., 2010. Pleistocene ice caps on the coastal mountains of the Adriatic Sea. *Quat. Sci. Rev.* 29 (27–28), 3690–3708. <https://doi.org/10.1016/j.quascirev.2010.06.032>.
- Jacobshagen, V. (Ed.), 1986. *Geologie von Griechenland*. Gebr. Borntraeger.
- Katsiviaris, N., Papazeti, E., Tsaila-Monoplaki, S., 2008. *Geological Map of Greece 1:50,000, Anoia Crete Sheet*. Institute of Geological and Mineral Exploration.
- Keserci, F., Bayrakdar, C., Çilgin, Z., Evans, I.S., 2023. Modeling the form, distribution and paleoclimatic implications of former glaciers in the Teke Peninsula (Eastern Mediterranean, Turkey). *Geomorphology* 431, 108683. <https://doi.org/10.1016/j.geomorph.2023.108683>.
- Kleman, J., Borgström, I., Skelton, A., Hall, A., 2016. Landscape evolution and landform inheritance in tectonically active regions: the case of the Southwestern Peloponnese, Greece. *Z. Geomorphol.* 60 (2), 171–193. <https://doi.org/10.1127/zfg/2016/0283>.
- Kutzbach, J.E., Chen, G., Cheng, H., Edwards, R., Liu, Z., 2014. Potential role of winter rainfall in explaining increased moisture in the Mediterranean and Middle East during periods of maximum orbitally-forced insolation seasonality. *Clim. Dyn.* 42, 1079–1095. <https://doi.org/10.1007/s00382-013-1692-1>.
- Lainé, A., Kageyama, M., Salas-Mélia, D., Voldoire, A., Rivière, G., Ramstein, G., Planton, S., Tyteca, S., Peterschmitt, J.-Y., 2009. Northern Hemisphere storm tracks during the last glacial maximum in the PMIP2 ocean-atmosphere coupled models:

- Energetic study, seasonal cycle, precipitation. *Clim. Dyn.* 32 (5), 593–614. <https://doi.org/10.1007/s00382-008-0391-9>.
- Lambeck, K., 1995. Late Pleistocene and Holocene sea-level change in Greece and southwestern Turkey: a separation of eustatic, isostatic, and tectonic contributions. *Geophys. J. Int.* 122 (3), 1022–1044. <https://doi.org/10.1111/j.1365-246X.1995.tb06853.x>.
- Leontaritis, A.D., 2021. *The Late Quaternary glacial History of Greece* (Doctoral Dissertation). Harokopio University of Athens, Greece. <https://doi.org/10.13140/RG.2.2.15282.02240>.
- Leontaritis, A.D., Pavlopoulos, K., Marrero, S.M., Ribolini, A., Hughes, P.D., Spagnolo, M., 2022. Glaciations on ophiolite terrain in the North Pindus Mountains, Greece: new geomorphological insights and preliminary ^{36}Cl exposure dating. *Geomorphology* 413, 108335. <https://doi.org/10.1016/j.geomorph.2022.108335>.
- Leontaritis, A.D., Kouli, K., Pavlopoulos, K., 2020. The glacial history of Greece: a comprehensive review. *Mediterranean Geoscience Reviews* 2, 65–90. <https://doi.org/10.1007/s42990-020-00021-w>.
- Li, H., Ng, F., Li, Z., Qin, D., Cheng, G., 2012. An extended “perfect-plasticity” method for estimating ice thickness along the flow line of mountain glaciers. *J. Geophys. Res.: Earth Surf.* 117 (F1), F01020. <https://doi.org/10.1029/2011JF002104>.
- Li, Y., 2023. PalaeoIc: an automated method to reconstruct palaeoglacier using geomorphic evidence and digital elevation models. *Geomorphology* 421, 108523. <https://doi.org/10.1016/j.geomorph.2022.108523>.
- Lilli, A.M., Efthathiou, D., Moraetis, D., Schuite, J., Nerantzaki, D.S., Nikolaidis, P.N., 2020. A multi-disciplinary approach to understand hydrologic and geochemical processes at Koiliaris Critical Zone Observatory. *Water* 12 (9), 2474. <https://doi.org/10.3390/w12092474>.
- Luetscher, M., Boch, R., Sodemann, H., Spötl, C., Cheng, H., Edwards, R.L., Frisia, S., Hof, F., Müller, W., 2015. North atlantic storm track changes during the last glacial maximum recorded by alpine speleothems. *Nat. Commun.* 6, 6344. <https://doi.org/10.1038/ncomms7344>.
- Maire, R., 1990a. Chapitre II. Deux hauts karsts du Péloponnèse (Taygète et Helmos). In: *La Haute Montagne Calcaire: Karsts, Cavités, Remplissages, Quaternaires, Paléoclimats*. Presses Universitaires de Bordeaux, pp. 179–302. <https://doi.org/10.4000/books.pub.11120>.
- Maire, R., 1990b. Chapitre III. Les hauts karsts de Crète (Ida et Levka Ori). In: *La Haute Montagne Calcaire: Karsts, Cavités, Remplissages, Quaternaires, Paléoclimats*. Presses Universitaires de Bordeaux, pp. 179–302. <https://doi.org/10.4000/books.pub.11126>.
- Marjanac, L., 2012. *Pleistocene Glacial and Periglacial Sediments of Kvarner, Northern Dalmatia and Southern Velebit Mts.-evidence of Dinaric Glaciation*. Prirodoslovno-matematički fakultet, Zagreb, pp. 245–256. Doctoral dissertation.
- Marjanac, T., Marjanac, L., 2016. The extent of middle Pleistocene ice cap in the coastal Dinaric Mountains of Croatia. *Quaternary Research* 85 (3), 445–455. <https://doi.org/10.1016/j.yqres.2016.03.006>.
- Mastronuzzi, G., Sanso, P., Stamatopoulos, L., 1994. *Glacial landforms of the peloponnese (Greece)*. Riv. Geogr. Ital. 101, 77–86.
- Matthews, J.A., Wilson, P., Mourne, R.W., 2017. Landform transitions from pronal ramparts to moraines and rock glaciers: a case study from the Smørbotn cirque, Romsdalsalpane, southern Norway. *Geografiska Annaler: Series B, Human Geography* 99 (1), 15–37. <https://doi.org/10.1080/04353676.2016.1256582>.
- McClusky, S., Balassanian, S., Barka, A., et al., 2000. Global Positioning System constraints on plate kinematics and dynamics in the eastern Mediterranean and Caucasus. *J. Geophys. Res.* 105 (B5695). <https://doi.org/10.1029/1999JB900351>.
- Messerli, B., 1967. Die eiszeitliche und die gegenwärtige Vergletscherung im Mittelmeerraum. *Geogr. Helv.* 22 (2), 105–228. <https://doi.org/10.5194/gh-22-105-1967>.
- Meulenkamp, J.E., van der Zwaan, G.J., van Wamel, W.A., 1994. On Late Miocene to recent vertical motions in the Cretan segment of the Hellenic arc. *Tectonophysics* 234, 53–72. [https://doi.org/10.1016/0040-1951\(94\)90204-6](https://doi.org/10.1016/0040-1951(94)90204-6).
- Mistardis, G., 1937. Sur la morphologie des parties supérieures des hautes montagnes de la Grèce. In: Reprinted from *Bulletin of the First Panhellenic Mountaineering Conference in Athens*, pp. 35–41.
- Monegato, G., Scardia, G., Hajdas, I., Rizzini, F., Piccin, A., 2017. The Alpine LGM in the boreal ice-sheets game. *Sci. Rep.* 7, 2078. <https://doi.org/10.1038/s41598-017-02148-7>.
- Moraetis, D., Leontaritis, A., Scharf, A., Fassoulas, C., Zacharias, S., Pavlopoulos, K., Mattern, F., Alnaqbi, A., Yu, X., Pennos, C., Adamopoulos, K., Hamdan, H., Nikolaidis, N.P., 2024. *A new geological model for the Lefka Ori Massif in the accretionary wedge of the Hellenic Subduction Zone (EGU24-9013)*. In: EGU General Assembly 2024. <https://doi.org/10.5194/egusphere-egu24-9013>. Vienna, Austria.
- Moraetis, D., Leontaritis, A., Scharf, A., Fassoulas, C., Zacharias, S., Malard, A., Mattern, F., Alnaqbi, A., Hamdan, H., Digenis, M., Pennos, C., Adamopoulos, K., Yu, X., Nikolaidis, N., Pavlopoulos, K., 2025. Preliminary hydrogeological implications using structural analysis and cave mapping: a case study of the pachnes thrust, central Lefka Ori, Crete episodes. <https://doi.org/10.18814/epiugs/2025/025015>.
- Moulin, A., Benedetti, L., Vidal, L., Hage-Hassan, J., Elias, A., Van der Woerd, J., Schimmeleppenig, I., Daëron, M., Tapponier, P., 2022. LGM glaciers in the SE Mediterranean? First evidence from glacial landforms and ^{36}Cl dating on Mount Lebanon. *Quat. Sci. Rev.* 285, 107502. <https://doi.org/10.1016/j.quascirev.2022.107502>.
- Mouslopoulou, V., Begg, J., Fülling, A., Moraetis, D., Partsinevelos, P., Oncken, O., 2017. Distinct phases of eustatic and tectonic forcing for late Quaternary landscape evolution in southwest Crete, Greece. *Earth Surf. Dyn.* 5, 511–527. <https://doi.org/10.5194/esurf-5-511-2017>.
- Mouslopoulou, V., Begg, J., Nicol, A., Oncken, O., Prior, C., 2015a. Formation of late quaternary paleoshorelines in crete, eastern mediterranean. *Earth Planet Sci. Lett.* 431, 294–307. <https://doi.org/10.1016/j.epsl.2015.09.007>.
- Mouslopoulou, V., Nicol, A., Begg, J., Oncken, O., Moreno, M., 2015b. Clusters of mega-earthquakes on upper plate faults control the Eastern Mediterranean hazard. *Geophys. Res. Lett.* 42, 10282–10289. <https://doi.org/10.1002/2015GL066371>, 6.
- Mouslopoulou, V., Oncken, O., Hainzl, S., Nicol, A., 2016. Uplift rate transients at subduction margins due to earthquake clustering. *Tectonics* 35, 2370–2384. <https://doi.org/10.1002/2016TC004248>.
- Nemec, W., Postma, G., 1993. Quaternary alluvial fans in southwestern Crete: sedimentation processes and geomorphic evolution. In: Marzo, M., Puigdefabregas, C. (Eds.), *Alluvial Sedimentation*. <https://doi.org/10.1002/9781444303995.ch18>.
- Nesje, A., 1992. Topographical effects on the equilibrium-line altitude on glaciers. *Geojournal* 27 (4), 383–391. <http://www.jstor.org/stable/41145524>.
- Niculescu, C., 1915. Sur les traces de glaciation dans le massif Smolica chaîne du Pinde méridional. *Bulletin de la Section des Sciences de l'Académie Roumaine* 3, 146–151.
- Ohmura, A., Boettcher, M., 2018. Climate on the equilibrium line altitudes of glaciers: Theoretical background behind Ahmann's P/T diagram. *J. Glaciol.* 64, 489–505. <https://doi.org/10.1017/jog.2018.41>.
- Osmaston, H.A., 2005. Estimates of glacier equilibrium line altitudes by the Area \times Altitude, the Area \times Altitude balance ratio and the Area \times Altitude balance index methods and their validation. *Quat. Int.* 138–139, 22–31. <https://doi.org/10.1016/j.quaint.2005.02.004>.
- Ott, R.F., Gallen, S.F., Wegmann, K.W., Biswas, R.H., Herman, F., Willett, S.D., 2019. Pleistocene terrace formation, Quaternary rock uplift rates, and geodynamics of the Hellenic Subduction Zone revealed from dating of paleoshorelines on Crete, Greece. *Earth Planet Sci. Lett.* 525, 115757. <https://doi.org/10.1016/j.epsl.2019.115757>.
- Ott, R.F., Scherler, D., Wegmann, K.W., D'Arcy, M.K., Pope, R.J., Ivy-Ochs, S., et al., 2023. Paleo-denudation rates suggest variations in runoff drove aggradation during the last glacial cycle, Crete, Greece. *Earth Surf. Process. Landf.* 48 (2), 386–405. <https://doi.org/10.1002/esp.5492>.
- Papanikolaou, D., Vassilakis, E., 2010. Thrust faults and extensional detachment faults in Cretan tectono-stratigraphy: implications for Middle Miocene extension. *Tectonophysics* 488, 233–247. <https://doi.org/10.1016/j.tecto.2009.06.024>.
- Pellittero, R., Rea, B.R., Spagnolo, M., Bakke, J., Hughes, P., Ivy-Ochs, S., Lukas, S., Ribolini, A., 2015. A GIS tool for automatic calculation of glacier equilibrium-line altitudes. *Comput. Geosci.* 82, 55–62. <https://doi.org/10.1016/j.cageo.2015.05.005>.
- Pellittero, R., Rea, B.R., Spagnolo, M., Bakke, J., Ivy-Ochs, S., Frew, C.R., Hughes, P., Ribolini, A., Lukas, S., Renssen, H., 2016. GlaRe: a GIS tool to reconstruct the 3D surface of palaeoglaciers. *Comput. Geosci.* 94, 77–85. <https://doi.org/10.1016/j.cageo.2016.06.008>.
- Peterreck, A., Schwarze, J., 2004. Architecture and Late Pliocene to recent evolution of outer-arc basins of the Hellenic subduction zone (south-central Crete, Greece). *J. Geodyn.* 38, 19–55. <https://doi.org/10.1016/j.jog.2004.03.002>.
- Pirazzoli, P.A., Laborel, J., Stiros, S.C., 1996. Earthquake clustering in the Eastern Mediterranean during historical times. *J. Geophys. Res.* 101, 6083–6097. <https://doi.org/10.1029/95JB00914>.
- Pirazzoli, P.A., Thommeret, J., Thommeret, J., Laborel, J., Montag-Gioni, L.F., 1982. Crustal block movements from holocene shorelines: Crete and antikythera (Greece). *Tectonophysics* 86, 27–43. [https://doi.org/10.1016/0040-1951\(82\)90060-9](https://doi.org/10.1016/0040-1951(82)90060-9).
- Pope, R.J., Hughes, P.D., Skourtos, E., 2017. Glacial history of mount chelmos, peloponnesus, Greece. In: Hughes, P.D., Woodward, J.C. (Eds.), *Quaternary Glaciation in the Mediterranean Mountains*, 433. Geological Society of London, pp. 211–236. <https://doi.org/10.1144/SP433.11>.
- Pope, R., Candy, I., Skourtos, E., 2016. A chronology of alluvial fan response to Late Quaternary sea level and climate change, Crete. *Quaternary Research* 86, 170–183. <https://doi.org/10.1016/j.yqres.2016.06.003>.
- Pope, R., Hughes, P.D., Woodward, J.C., Noble, S., Sahy, D., Skourtos, E., et al., 2023. Long-term glacial and fluvial system coupling in southern Greece and evidence for glaciation during Marine Isotope Stage 16. *Quat. Sci. Rev.* 317, 108239. <https://doi.org/10.1016/j.quascirev.2023.108239>.
- Pope, R., Wilkinson, K., Skourtos, E., Triantaphyllou, M., Ferrier, G., 2008. Clarifying stages of alluvial fan evolution along the Sfakian piedmont, southern Crete: new evidence from analysis of post-incisive soils and OSL dating. *Geomorphology* 94, 206–225. <https://doi.org/10.1016/j.geomorph.2007.05.007>.
- Poser, J., 1957. *Klimamorphologische Probleme auf Kreta*. *Z. Geomorphol.* 2, 113–142.
- Price, S., Higham, T., Nixon, L., Moody, J., 2002. Relative sea-level changes in Crete: reassessment of radiocarbon dates from Sphakia and west Crete. *Annu. Br. Sch. A. T. Athens* 97, 171–200. <https://doi.org/10.1017/S0068245400017378>.
- Rackham, O., Moody, J., 1996. *The Making of the Cretan Landscape*. Manchester University Press.
- Rasmussen, S.O., Andersen, K.K., Svensson, A.M., et al., 2006. A new Greenland ice core chronology for the last glacial termination. *J. Geophys. Res.* 111. <https://doi.org/10.1029/2005JD006079>.
- Rasmussen, S.O., Bigler, M., Blockley, S.P., et al., 2014. A stratigraphic framework for abrupt climatic changes during the Last Glacial period based on three synchronized Greenland ice-core records: Refining and extending the INTIMATE event stratigraphy. *Quat. Sci. Rev.* 106, 14–28. <https://doi.org/10.1016/j.quascirev.2014.09.007>.
- Rea, B.R., 2009. Defining modern-day area-altitude balance ratios (AABRs) and their use in glacier-climate reconstructions. *Quat. Sci. Rev.* 28 (3–4), 237–248. <https://doi.org/10.1016/j.quascirev.2008.10.011>.
- Rea, B.R., Pellittero, R., Spagnolo, M., Hughes, P., Ivy-Ochs, S., Renssen, H., Ribolini, A., Bakke, J., Lukas, S., Braithwaite, R.J., 2020. Atmospheric circulation over Europe

- during the younger dryas. *Sci. Adv.* 6 (50), eaba4844. <https://doi.org/10.1126/sciadv.aba4844>.
- Roberts, G.G., White, N.J., Shaw, B., 2013. An uplift history of Crete, Greece, from inverse modeling of longitudinal river profiles. *Geomorphology* 198, 177–188. <https://doi.org/10.1016/j.geomorph.2013.05.026>.
- Robertson, J., Roberts, G.P., Ganas, A., Meschis, M., Gheorghiu, D.M., Shanks, R.P., 2023. Quaternary uplift of palaeoshorelines in southwestern Crete: the combined effect of extensional and compressional faulting. *Quat. Sci. Rev.* 316, 108240. <https://doi.org/10.1016/j.quascirev.2023.108240>.
- Ruddiman, W.F., McIntyre, A., 1981a. The mode and mechanism of the last deglaciation: Oceanic evidence. *Quaternary Research* 16 (2), 125–134. [https://doi.org/10.1016/0033-5894\(81\)90040-5](https://doi.org/10.1016/0033-5894(81)90040-5).
- Ruddiman, W.F., McIntyre, A., 1981b. The North atlantic ocean during the last deglaciation. *Palaeogeogr. Palaeoclimatol. Palaeoecol.* 35 (2–4), 145–214. [https://doi.org/10.1016/0031-0182\(81\)90097-3](https://doi.org/10.1016/0031-0182(81)90097-3).
- Sarikaya, M.A., Çiner, A., 2017. The late Quaternary glaciation in the eastern Mediterranean. In: Hughes, P., Woodward, J. (Eds.), *Quaternary Glaciation in the Mediterranean Region*, 433. Geological Society of London, Special Publications, pp. 289–305. <https://doi.org/10.1144/SP433.4>.
- Sarikaya, M.A., Çiner, A., Haybat, H., Zreda, M., 2014. An early advance of glaciers on Mount Akdağ, SW Turkey, before the global Last Glacial Maximum: insights from cosmogenic nuclides and glacier modeling. *Quat. Sci. Rev.* 88, 96–109. <https://doi.org/10.1016/j.quascirev.2014.01.016>.
- Sarikaya, M.A., Zreda, M., Çiner, A., Zweck, C., 2008. Cold and wet Last Glacial Maximum on Mount Sandras, SW Turkey, inferred from cosmogenic dating and glacier modeling. *Quat. Sci. Rev.* 27 (7–8), 769–780. <https://doi.org/10.1016/j.quascirev.2008.01.002>.
- Shaw, B., Ambraseys, N.N., England, P.C., Floyd, M.A., Gorman, G.J., Higham, T.F.G., Jackson, J.A., Nocquet, J.-M., Pain, C.C., Piggott, M.D., 2008. Eastern Mediterranean tectonics and tsunami hazard inferred from the AD365 earthquake. *Nat. Geosci.* 1, 268–276. <https://doi.org/10.1038/ngeo151>.
- Stamatilis, F., Nikolaidis, N., Vozinakis, K., Papamastorakis, D., Kritsotakis, M., 2006. Stochastic modeling of the karstic system of western Apokoronas in Crete. Chania, Greece. In: *Proceedings of the VIII International Conference on Protection and Restoration of the Environment*, pp. 184–192. vol. VIII.
- Styllas, M.N., Schimmelpfennig, I., Benedetti, L., Ghilardi, M., Aumaître, G., Bourlès, D., Keddadouche, K., 2018. Late-glacial and Holocene history of the Northeast Mediterranean mountain glaciers - new insights from in situ-produced ^{36}Cl -based cosmic ray exposure dating of paleo-glacier deposits on Mount Olympus, Greece. *Quat. Sci. Rev.* 193, 244–265. <https://doi.org/10.1016/j.quascirev.2018.06.020>.
- Tiberti, M., Basili, R., Vannoli, P., 2014. Ups and downs in western Crete (Hellenic subduction zone). *Sci. Rep.* 4, 5677. <https://doi.org/10.1038/srep05677>.
- Tzoraki, O., Kritsotakis, M., Baltas, E., 2015. Spatial water use efficiency index towards resource sustainability: Application in the island of Crete, Greece. *Int. J. Water Resour. Dev.* 31 (4), 669–681. <https://doi.org/10.1080/07900627.2014.949637>.
- van Hinsbergen, D.J.J., Meulenkamp, J.E., 2006. Neogene supradetachment basin development on Crete (Greece) during exhumation of the South Aegean core complex. *Basin Res.* 18, 103–124. <https://doi.org/10.1111/j.1365-2117.2005.00282.x>.
- Vidakis, M., Triantaphyllis, M., Mylonakis, I., 1993. Geological Map of Greece (1/50,000), Vrisses Sheet. The Institute of Geology and Mineral Exploration of Greece (I.G.M.E., Athens).
- Vogiatzakis, I.N., Griffiths, G.H., Mannion, A.M., 2003. Environmental Factors and Vegetation Composition, Lefka Ori Massif, Crete, S. Aegean, 12. Global Ecology & Biogeography, pp. 131–146. <https://doi.org/10.1046/j.1466-822X.2003.00021.x>.
- Wagner, B., Vogel, H., Francke, A., others, 2019. Mediterranean winter rainfall in phase with African monsoons during the past 1.36 million years. *Nature* 573, 256–260. <https://doi.org/10.1038/s41586-019-1529-0>.
- Woodward, J.C., Hughes, P.D., 2011. Glaciation in Greece: a new record of cold stage environments in the Mediterranean. In: Ehlers, J., Gibbard, P.L., Hughes, P.D. (Eds.), *Quaternary Glaciations - Extent and Chronology: A Closer Look*. Elsevier, pp. 175–198. <https://doi.org/10.1016/B978-0-444-53447-7.00015-5>.
- Woodward, J.C., Macklin, M.G., Smith, G.R., 2004. Pleistocene glaciation in the mountains of Greece. In: Ehlers, J., Gibbard, P.L. (Eds.), *Quaternary Glaciations - Extent and Chronology. Part I: Europe*. Elsevier, pp. 155–173. [https://doi.org/10.1016/S1571-0866\(04\)80066-6](https://doi.org/10.1016/S1571-0866(04)80066-6).
- Zacharias, S., Papadakos, P., Digenis, M., Margiolis, A., Tsopelas, M., Psomas, M., Mavrokosta, C., Apokoroniatis, A., Kostidis, K., Papamathaiaki, I., Soultatos, I., Adamopoulos, K., 2022. Sternes: the deep cave in the White Mountains (Lefka Ori) of Crete (Greece), still attracting cave explorers. vol. II. In: *Proceedings of the 18th International Congress of Speleology, Savoie 2022*, pp. 197–200. *Karstologia Memoires No. 22, Caving and explorations*.
- Zimmer, P.D., Gabet, E.J., 2018. Assessing glacial modification of bedrock valleys using a novel approach. *Geomorphology* 318, 336–347. <https://doi.org/10.1016/j.geomorph.2018.06.021>.
- Aris Leontaritis is the Principal Investigator and his contribution spans from the conceptualization of this research, organization and conduction of field surveys, securing the necessary funds, creation of maps, diagrams and pictures to writing the manuscript.
- Daniel Moraetis also took part in the conceptualization of this research and was very actively involved in the organization and conduction of field surveys as well as in securing the necessary funds. He also reviewed the paper and partly participated in writing the manuscript.
- Kosmas Pavlopoulos also took part in the conceptualization of this research and was partly involved in the organization and conduction of field surveys as well as in securing the necessary funds. He also reviewed the paper and partly participated in writing the manuscript.
- Phil Hughes reviewed the paper and partly participated in writing the manuscript.
- Charalampos Fassoulas was partly involved in the organization and conduction of field surveys as well as in securing the necessary funds. He also reviewed the paper and partly participated in writing the manuscript.